



**HAL**  
open science

## The epigenetic regulator RINF (CXXC5) maintains SMAD7 expression in human immature erythroid cells and sustains red blood cell expansion

Audrey Astori, Gabriel Matherat, Isabelle Munoz, Emilie-Fleur Gautier, Didier Surdez, Yaël Zermati, Frédérique Verdier, Sakina Zaidi, Vincent Feuillet, Amir Kadi, et al.

### ► To cite this version:

Audrey Astori, Gabriel Matherat, Isabelle Munoz, Emilie-Fleur Gautier, Didier Surdez, et al.. The epigenetic regulator RINF (CXXC5) maintains SMAD7 expression in human immature erythroid cells and sustains red blood cell expansion. *Haematologica*, 2020, 107, pp.268-283. 10.3324/haematol.2020.263558 . hal-03876291

**HAL Id: hal-03876291**

**<https://hal.science/hal-03876291>**

Submitted on 28 Nov 2022

**HAL** is a multi-disciplinary open access archive for the deposit and dissemination of scientific research documents, whether they are published or not. The documents may come from teaching and research institutions in France or abroad, or from public or private research centers.

L'archive ouverte pluridisciplinaire **HAL**, est destinée au dépôt et à la diffusion de documents scientifiques de niveau recherche, publiés ou non, émanant des établissements d'enseignement et de recherche français ou étrangers, des laboratoires publics ou privés.



Distributed under a Creative Commons Attribution - NonCommercial 4.0 International License



Ferrata Storti Foundation

# The epigenetic regulator RINF (CXXC5) maintains SMAD7 expression in human immature erythroid cells and sustains red blood cell expansion

Audrey Astori,<sup>1,2,3\*</sup> Gabriel Matherat,<sup>1,2,3\*</sup> Isabelle Munoz,<sup>1,2,3</sup> Emilie-Fleur Gautier,<sup>1,2,3</sup> Didier Surdez,<sup>3,4,5</sup> Yaël Zermati,<sup>1,2</sup> Frédérique Verdier,<sup>1,2</sup> Sakina Zaidi,<sup>3,4,5</sup> Vincent Feuillet,<sup>1</sup> Amir Kadi,<sup>1</sup> Evelyne Lauret,<sup>1,3</sup> Olivier Delattre,<sup>3,4,5</sup> Carine Lefèvre,<sup>1,2</sup> Michaela Fontenay,<sup>1,2,6</sup> Evelyne Ségal-Bendirdjian,<sup>7</sup> Isabelle Dusanter-Fourt,<sup>1,3</sup> Didier Bouscary,<sup>1,3</sup> Olivier Hermine,<sup>2,3,8</sup> Patrick Mayeux<sup>1,2,3</sup> and Frédéric Pendino<sup>1,2,3</sup>

Haematologica 2022  
Volume 107(1):268-283

<sup>1</sup>Université de Paris, Institut Cochin, INSERM, CNRS; <sup>2</sup>Laboratory of Excellence GR-ex; <sup>3</sup>Equipe Labellisée Ligue Nationale Contre le Cancer (LNCC); <sup>4</sup>PSL Research University, Institut Curie Research Center, INSERM U830; <sup>5</sup>SIREDO: Care, Innovation and Research for Children, Adolescents and Young Adults with Cancer, Institut Curie; <sup>6</sup>Service d'Hématologie Biologique, Hôpital Cochin, Assistance Publique-Hôpitaux de Paris, Centre-Université de Paris; <sup>7</sup>INSERM UMR-S 1124, Team: Cellular Homeostasis Cancer and Therapies, Université de Paris and <sup>8</sup>Université de Paris, Institut Imagine, INSERM, CNRS, Paris, France.

\*AA and GM contributed equally as co-first authors.

## ABSTRACT

The gene *CXXC5*, encoding a retinoid-inducible nuclear factor (RINF), is located within a region at 5q31.2 commonly deleted in myelodysplastic syndrome and adult acute myeloid leukemia. RINF may act as an epigenetic regulator and has been proposed as a tumor suppressor in hematopoietic malignancies. However, functional studies in normal hematopoiesis are lacking, and its mechanism of action is unknown. Here, we evaluated the consequences of *RINF* silencing on cytokine-induced erythroid differentiation of human primary CD34<sup>+</sup> progenitors. We found that *RINF* is expressed in immature erythroid cells and that *RINF*-knockdown accelerated erythropoietin-driven maturation, leading to a significant reduction (~45%) in the number of red blood cells, without affecting cell viability. The phenotype induced by *RINF*-silencing was dependent on tumor growth factor  $\beta$  (TGF $\beta$ ) and mediated by SMAD7, a TGF $\beta$ -signaling inhibitor. RINF upregulates SMAD7 expression by direct binding to its promoter and we found a close correlation between *RINF* and SMAD7 mRNA levels both in CD34<sup>+</sup> cells isolated from bone marrow of healthy donors and myelodysplastic syndrome patients with del(5q). Importantly, RINF knockdown attenuated SMAD7 expression in primary cells and ectopic SMAD7 expression was sufficient to prevent the *RINF* knockdown-dependent erythroid phenotype. Finally, *RINF* silencing affects 5'-hydroxymethylation of human erythroblasts, in agreement with its recently described role as a TET2-anchoring platform in mouse. Collectively, our data bring insight into how the epigenetic factor RINF, as a transcriptional regulator of SMAD7, may fine-tune cell sensitivity to TGF $\beta$  superfamily cytokines and thus play an important role in both normal and pathological erythropoiesis.

## Correspondence:

FRÉDÉRIC PENDINO  
frederic.pendino@inserm.fr

Received: June 18, 2020.

Accepted: November 16, 2020.

Pre-published: November 26, 2020.

<https://doi.org/10.3324/haematol.2020.263558>

©2022 Ferrata Storti Foundation

Material published in *Haematologica* is covered by copyright. All rights are reserved to the Ferrata Storti Foundation. Use of published material is allowed under the following terms and conditions:

<https://creativecommons.org/licenses/by-nc/4.0/legalcode>.

Copies of published material are allowed for personal or internal use. Sharing published material for non-commercial purposes is subject to the following conditions:

<https://creativecommons.org/licenses/by-nc/4.0/legalcode>,

sect. 3. Reproducing and sharing published material for commercial purposes is not allowed without permission in writing from the publisher.



## Introduction

In earlier work, we demonstrated that *RINF* loss-of-function affects granulopoiesis in normal and tumoral human hematopoietic cells.<sup>1</sup> In keeping with its gene location at chromosome 5q31.2 (*Online Supplementary Figure S1*), a commonly deleted region associated with high risk in myeloid neoplasms,<sup>2</sup> *RINF* loss of expression has been

proposed to contribute to the development or progression of (pre)leukemia, such as myelodysplastic syndrome (MDS).<sup>1,3,5</sup> We and others have demonstrated that *RINF* mRNA expression is an unfavorable<sup>6,7</sup> and independent<sup>3</sup> prognostic factor in acute myeloid leukemia (AML) as well as in solid tumors.<sup>8,9</sup> However, its role in normal hematopoiesis has hitherto been poorly investigated and its contribution to the erythroid lineage and red blood cell (RBC) expansion is unknown.

RINF contains a nuclear localization signal that has been functionally validated<sup>10</sup> and, in most studies, its subcellular localization is reported to be mainly or exclusively nuclear and it acts as a transcriptional cofactor.<sup>1,3,8,10-17</sup> RINF associates strongly with chromatin<sup>1</sup> through its conserved zinc-finger domain (CXXC) which plays an essential role in providing the capacity to bind CpG islands.<sup>18,19</sup> Interestingly, this domain is almost identical to the one harbored by TET1 and TET3, two epigenetic modulators involved in the erasure of DNA-methylation marks,<sup>20</sup> pointing to the possibility that RINF might interfere with TET activities, hydroxymethylation, and gene transcription, as recently demonstrated in mice.<sup>12,15</sup> RINF has also been reported to bind ATM, mediate DNA-damage-induced activation of TP53<sup>3,10</sup> and inhibit the WNT- $\beta$ -catenin signaling pathway<sup>3,21-24</sup> through a cytoplasmic interaction with disheveled proteins DVL and DVL2.<sup>21</sup>

Transforming growth factor  $\beta$  (TGF $\beta$ ) is a powerful and widespread cell growth inhibitor in numerous mammalian tissues.<sup>25,26</sup> In the hematopoietic system, TGF $\beta$  is known to regulate hematopoietic stem and progenitor cells (HSPC) and is also described as a potent inducer of erythroid differentiation and inhibitor of cell proliferation.<sup>27-30</sup> TGF $\beta$  signals through cell surface serine/threonine kinase receptors, mainly TGF $\beta$ RI and TGF $\beta$ RII. Activated TGF $\beta$ RI phosphorylates SMAD2 and SMAD3 which translocate into the nucleus and form complexes that regulate transcription of target genes. TGF $\beta$  can also elicit its biological effects by activation of SMAD-independent pathways.<sup>31,32</sup> Inhibitory SMAD (SMAD6 and SMAD7) inhibit TGF $\beta$  signaling. Importantly, a reduced *SMAD7* expression sensitizes cells to the antiproliferative effects of TGF $\beta$  and contributes to anemia in patients suffering from MDS, suggesting, firstly, that identifying transcriptional regulators of *SMAD7* could enlighten our understanding of erythropoiesis and, secondly, that inhibiting TGF $\beta$  signaling could be a therapeutic strategy that would mitigate ineffective hematopoiesis in disease states.<sup>33-35</sup>

In the present work, we used primary human CD34<sup>+</sup> cells to demonstrate that RINF knockdown affects human erythropoiesis and mitigates RBC production through a mechanism that is mediated by SMAD7, the main inhibitor of TGF $\beta$  signaling.

## Methods

The methods for flow cytometric cell sorting of megakaryocyte-erythroid progenitor (MEP) cells, immunofluorescence studies, chromatin Immunoprecipitation (ChIP) experiments, and the primer sequences used for quantitative reverse transcriptase polymerase chain reaction (qRT-PCR) and ChIP-qPCR are described in the *Online Supplementary Methods*.

### Primary culture of hematopoietic cells

Mononuclear cells were isolated from cord blood (CRB Saint-

Louis Hospital, Paris, France) or adult bone marrow donors with written informed consent for research use, in accordance with the Declaration of Helsinki. The ethics evaluation committee of INSERM, the Institutional Review Board (IRB00003888), approved our research project (n. 16-319). Mononucleated cells were separated by Ficoll-Paque (Life Technologies) and purified with a human CD34 MicroBead Kit (cat. n. 130100453, Miltenyi Biotec). A two-step culture method for cell expansion and erythroid differentiation was used to obtain highly stage-enriched erythroblast populations.<sup>36,37</sup> Briefly, CD34<sup>+</sup> cells (purity 94-98%) were cultured for 7 days with interleukin (IL)6, IL3 (10 ng/mL), and stem cell factor (SCF, 100 ng/mL) to expand hematopoietic progenitors.<sup>37</sup> CD36<sup>+</sup> erythroid progenitors were purified using magnetic microbeads (CD36 FA6.152 from Beckman Coulter and anti-mouse IgG1 MicroBeads from Miltenyi Biotec). Then, erythropoietin (EPO) was added for 10-18 days to allow erythroid differentiation. For assays of colony-forming cells (CFC, counted at 11-14 days), CD34<sup>+</sup> hematopoietic stem cells were seeded in methylcellulose (H4034, StemCell Technologies). TGF $\beta$ RI inhibitor SB431542 was from Selleckchem (cat. n. S1067)<sup>38</sup> and TGF $\beta$  was from Peprotech (cat. n. 100-21).

### Flow cytometry and differentiation analysis

To monitor end-stage erythroid differentiation of primary cells, cells were labeled with anti-human PE/Cy7-conjugated glycophorin A (GPA/CD235a) (cat n. A71564), PE-conjugated CD71 (IM2001U), and APC-conjugated CD49d (cat. n. B01682) from Beckman Coulter, PE-conjugated CD233/Band3 from IBGRL (cat. n. 9439-PE). Fluorescence-activated cell sorting (FACS) analysis was performed on an Accuri<sup>TM</sup> C6 Flow Cytometer (Becton-Dickinson). For morphological characterization cells were cytopun and stained with May-Grünwald-Giemsa. For the benzidine assay,  $2 \times 10^5$  cells were incubated for 5 min with 0.01% benzidine and H<sub>2</sub>O. at 0.3% (Sigma-Aldrich).

### Culture of cell lines and treatments

K562 (ATCC#CCL243) and UT7.<sup>39</sup> cells were cultured in RPMI 1640 medium and minimum essential medium- $\alpha$  supplemented with 2.5 ng/mL of granulocyte-macrophage colony-stimulating factor (GM-CSF; Miltenyi Biotec), respectively. Both media were supplemented with 10% inactivated fetal bovine serum, 2 mM L-glutamine, 50 U/mL penicillin G and 50  $\mu$ g/mL streptomycin (Life Technologies). To induce hemoglobin production, K562 cells were treated with hemin at 40  $\mu$ M (Sigma-Aldrich). Erythroid maturation of UT7.<sup>39</sup> was triggered by replacing GM-CSF with EPO 5 U/mL.

### Lentiviral and retroviral transduction of hematopoietic cells

For shRNA-mediated RINF knockdown, we used the pTRIPDU3/GFP lentiviral vector<sup>40</sup> which drives the same shRNA sequences downstream of the H1 promoter as our previously described pLKO.1/puroR vector.<sup>1</sup> For *RINF* overexpression, the retroviral vector MigR/IRES-GFP was used with the previously described experimental conditions.<sup>1</sup> Green fluorescent protein (GFP) sorting was performed on a FACS Aria III (BD Biosciences). For *SMAD7* overexpression, the retroviral vector pBABE-puro-*SMAD7-HA* (Addgene plasmid#37044) was used as previously described.<sup>1,41</sup> For doxycycline-inducible lentiviral expression, *SMAD7-HA* cDNA was inserted into the pINDUCER21 vector by gateway technology (Addgene plasmid #46948) and shRNA sequences were inserted in the Tet-pLKO-GFP vector (modified from Tet-pLKO-puro, Addgene plasmid#21915, deposited by Dmitri Wiederschain).

## Quantitative reverse transcriptase polymerase chain reaction

Cells were collected and stored directly at  $-80^{\circ}\text{C}$  for RNA preparation with the TRIzol (Life Technologies) extraction protocol as previously described.<sup>1</sup> First-strand cDNA synthesis (reverse transcription) was carried out using a Transcriptor First Strand cDNA Synthesis Kit (cat. n. 489703000, Roche). *RINF* mRNA expression was detected using a Lightcycler<sup>®</sup> 480 ProbesMaster kit (cat. n. 4707494001, Roche). Relative mRNA expression was normalized to *RLPL2*, *PPIA* or *ACTB* gene expression in a two-color duplex reaction. For *SMAD7*, *PU.1* and *c-KIT* mRNA detection, qRT-PCR was performed using SYBRGreen on a Light Cycler 480 machine (Roche) and gene expression was calculated by the  $2^{-\Delta\Delta\text{CT}}$  method. Primer sequences are available in an *Online Supplementary File*.

## Western blot analysis

Total cell extracts were prepared and western blotting was carried out as previously described.<sup>1</sup> Blots were incubated with a primary polyclonal antibody and then with an appropriate peroxidase-conjugated secondary antibody (anti-rabbit and anti-mouse IgG horseradish peroxidase [HRP] antibodies from Cell Signaling, cat. n. 7074S, and 7076S, respectively) and anti-goat IgG HRP antibody from Southern Biotech (cat. n. 6160-05). Proteins were detected using a chemiluminescent system (Clarity Western ECL, cat. n. 170-5060, Biorad). Rabbit polyclonal antibodies were previously described for *RINF*,<sup>1</sup> P85/PI3KR1,<sup>42</sup> or commercially purchased for anti-*RINF*, anti-*SMAD7* (cat. n. 16513-1-AP, cat. n. 25840-1-AP, ProteinTech), anti- $\beta$ -actin (*ACTB*, cat. n. A1978, Sigma-Aldrich), anti-phospho-*SMAD2/3* (cat. n. 8828, Cell Signaling), and anti-HSC70 mouse monoclonal antibody (SC-7298, Santa Cruz Biotechnology).

## Statistical analyses

All analyses were performed using GraphPad Prism software. When the distribution of data was normal, the two-tailed Student *t* test was used for group comparisons. Contingency tables were established using the Fisher exact test, and the Pearson correlation coefficient was used to determine the correlation between the normally distributed *RINF* mRNA and *SMAD7* mRNA expression values. Statistics were carried out on a minimum of three independent experiments. The statistical significance of *P* values is indicated in the Figures: not significant (ns):  $P>0.05$ ; \* $P<0.05$ ; \*\* $P<0.01$ ; \*\*\* $P<0.001$ . Error bars represent confidence intervals at 95% or standard deviations (SD) for the qRT-PCR analyses.

## Results

### *RINF* is expressed during early human erythropoiesis

We employed cytokine-induced erythroid differentiation of CD34<sup>+</sup> progenitor cells isolated from human cord blood or adult bone marrow to model human erythropoiesis *in vitro*. To obtain highly enriched populations of differentiating erythroblasts, cells were grown in a two-phase liquid culture (experimental design in Figure 1A) as previously described.<sup>36,37</sup> We found that *RINF* protein was present at the earliest stages of erythroid differentiation and reached its highest level in progenitors and proerythroblasts (ProE) (Figure 1B). After that, the level of *RINF* protein decreased in the basophilic erythroblast stage and was barely detectable in late erythroblasts (i.e., polychromatic and orthochromatic erythroblast stages). Similarly, *RINF* mRNA levels were high in erythroid progenitors but decreased at

the basophilic stage and onwards (Figure 1C). This temporal expression pattern mirrors *RINF* expression data extracted from three independent transcriptome datasets (microarray or RNA-sequencing) reported by Merryweather-Clarke et al.,<sup>43</sup> An et al.,<sup>44</sup> and Keller et al.<sup>45</sup> with adult or cord-blood CD34<sup>+</sup> cells (*Online Supplementary Figure S2*). Taken together, our data show that *RINF* expression peaks in erythroid progenitors and proerythroblasts during cytokine-induced erythropoiesis.

### *RINF* silencing results in diminished red blood cell production without affecting cell viability

We next investigated the consequences of *RINF* knockdown on erythropoiesis and cell viability (see experimental design in Figure 2A). Knockdown experiments were performed with two previously validated short-hairpin RNA (*shRINF#4* and *shRINF#3*) sequences<sup>1</sup> driven by the lentiviral pTRIPDU3/GFP vector (*Online Supplementary Figure S3A, B*). We found that *RINF* was extinguished as early as 2 days after transduction (i.e., at day 0 of EPO) with *shRINF#4* at both mRNA (Figure 2B) and protein (Figure 2C) levels, without affecting cell viability, assessed by trypan blue cell counting (Figure 2D) or cell growth up to day 10 of EPO (Figure 2E, left panel). However, in the last days of *ex vivo* culture (day 11-17), we noticed a reduction in total number of RBC produced (average decrease of ~45%) at 17 days with EPO (Figure 2E, right panel), which was particularly marked for four donors out of six studied.

To investigate how *RINF* knockdown affects the clonogenic capacity of HSPC, we next performed comparative colony-forming assays for the development and maturation of erythroid (burst-forming unit erythroid progenitors; BFU-E), myeloid (CFU-G, CFU-M, or CFU-GM) and mixed (CFU-GEMM) colonies. No statistically significant changes were noted in the total number of colonies or the number of CFU-M, CFU-GM, or CFU-GEMM (*Online Supplementary Figure S3C*). However, the proportions of granulocytic colonies (CFU-G) and BFU-E, were slightly reduced or increased, respectively ( $P<0.01$ , Fisher exact test). The number of MEP-sorted cells was also increased under *RINF* knockdown conditions (*Online Supplementary Figure S3E*), and this increase corresponded with an increase in small (more mature) BFU-E, findings that suggest an accelerated maturation. A more careful analysis of colony size revealed that the median size of BFU-E derived from CD34<sup>+</sup> cells dropped by about 30% (i.e., from 0.101 to 0.071 mm<sup>2</sup>, unpaired *t*-test,  $P=0.007$ ,  $n=3$  donors) after *RINF* knockdown (Figure 2F). Concomitantly with the size reduction of large BFU-E (the most immature ones), we noted a slight but statistically significant increase in small BFU-E (the most mature ones), in agreement with accelerated maturation (Figure 2G).

### Erythroid maturation is affected by *RINF*

We next investigated whether the reduced expansion observed from day 10 of EPO could be the consequence of accelerated maturation. Indeed, we observed that erythroid differentiation was accelerated under conditions of *RINF* knockdown using quantification by benzidine staining (Figure 3A), morphological analysis of cells stained with May-Grünwald-Giemsa (Figure 3B), and flow cytometry for the erythroid markers GPA and CD71 (Figure 3C, upper panel), and CD49d and Band3 (Figure 3C, lower panel). These differences were statistically significant ( $P<0.001$ ) for CD34<sup>+</sup> cells derived from both cord

blood and adult bone marrow. The shRNA-RINF-induced acceleration of erythropoiesis was supported by the reduction in cell size (*not shown*) and the more rapid downregulation of *c-KIT* and *PU.1* mRNA in *RINF* knockdown cells (Figure 3D). The accelerated maturation was also characterized by a pronounced reduction of ProE cells (~2.8-fold less) enumerated at day 11 (Figure 3B). Despite a weaker efficiency of *shRINF#3* to knockdown *RINF* expression compared to *shRINF#4* (Online Supplementary Figure S3B, Figure 3E, left panel), we also confirmed that a similar phenotype, i.e., accelerated maturation (as shown by increased benzidine staining) (Figure 3E, right panel) and a reduction in the total num-

ber of RBC produced at day 17 (Figure 3F), was obtained with another shRNA sequence targeting *RINF*.

**RINF controls erythroid maturation and red blood cell expansion in a transforming growth factor  $\beta$ -dependent manner**

We then wondered whether TGF $\beta$ , a well-known inducer of erythroid maturation and inhibitor of RBC expansion, could be involved in the RINF-dependent phenotype. In agreement with an important role for autocrine TGF $\beta$  signaling in the early stages of erythropoiesis, both TGF $\beta$ 1 and TGF $\beta$ RI were highly expressed in erythroid progenitors (Figure 4A). To functionally validate an involvement of the

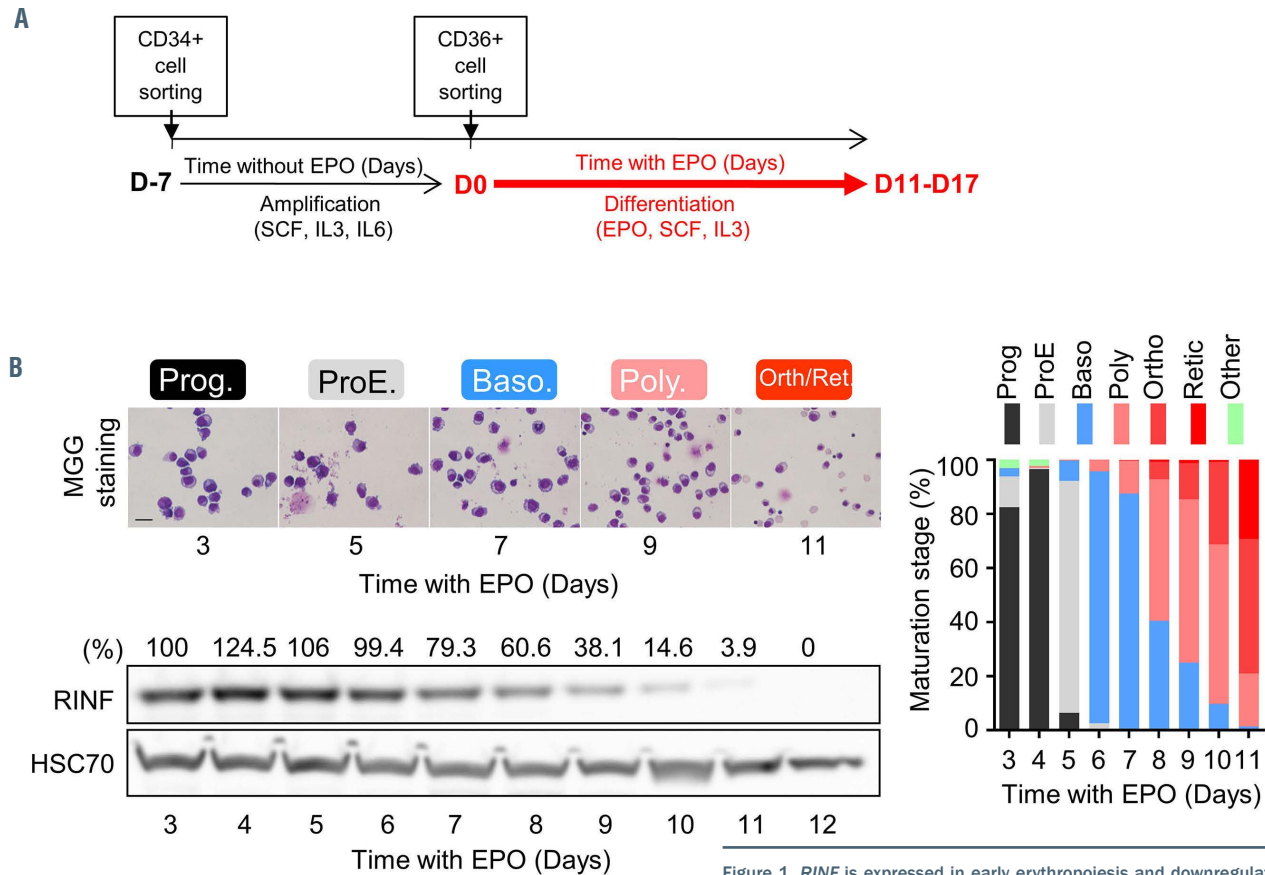


**Figure 1.** *RINF* is expressed in early erythropoiesis and downregulated during maturation of human hematopoietic stem and progenitor cells. (A) Schematic representation of cell culture experiments. CD34<sup>+</sup> cells (from cord blood or adult bone marrow) were first amplified for 7 days (D-7 to D0, in black) in the presence of stem cell factor (SCF), interleukin-3 (IL3) and interleukin-6 (IL6). Cells were sorted for CD36 expression and erythropoietin (EPO) was added to the medium in order to trigger the late stage of erythropoiesis, a phase lasting 11-17 days (in red). (B) For morphological characterization, cells were cytospun and stained with May-Grünwald-Giemsa (MGG) and the repartition of cells among differentiation stages indicated in percentages (right panel): early progenitor (Prog), proerythroblast (ProE), early and late basophilic erythroblast (Baso), polychromatophilic erythroblast (Poly), orthochromatic erythroblast (Ortho), and reticulocyte (Retic). The scale bar represents 20  $\mu$ m. The experiment presented here is representative of four distinct experiments which were performed on cells isolated from human cord blood. *RINF* protein was detected by western-blot analysis (lower panel). HSC70 protein was used as a loading control. For each lane, 40  $\mu$ g of protein were loaded. Band intensities were quantified with the Multigauge software and the relative expression of *RINF* protein (normalized to the loading control) is indicated above the image in percentages on day 3. (C) *CXXC5* mRNA expression was measured by quantitative reverse transcriptase polymerase chain reaction (qRT-PCR). *CXXC5* mRNA expression is downregulated from the basophilic erythroblast stage. Here, CD34<sup>+</sup> cells were isolated from adult human bone marrow, but a similar expression profile was observed with cells isolated from cord blood.

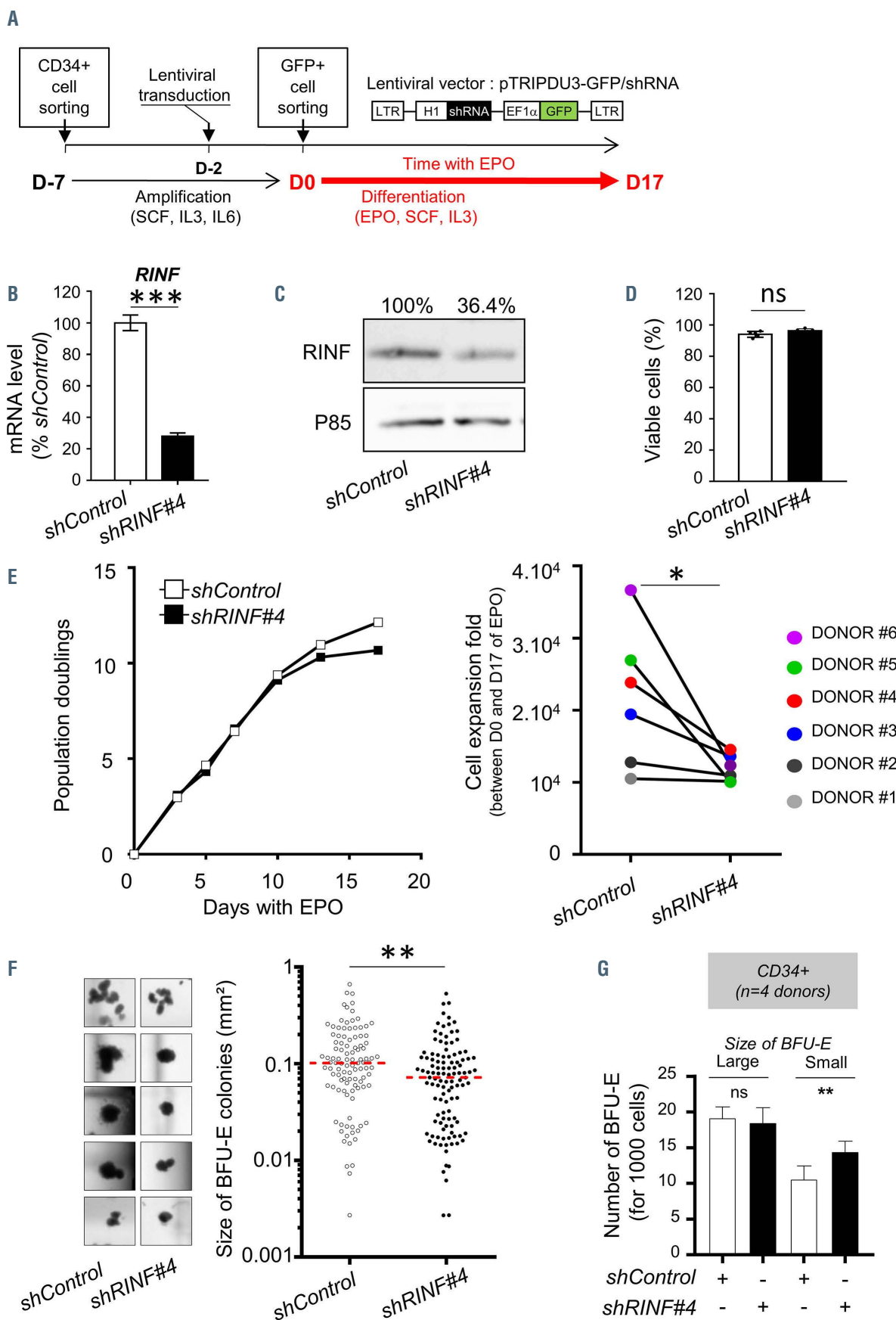


Figure 2. Legend on following page.

**Figure 2.** *RINF* knockdown leads to a reduction in total number of red blood cells generated from human hematopoietic stem and progenitor cells. (A) Schematic representation of the shRNA-mediated *RINF* loss of expression experiment. CD34<sup>+</sup> cells isolated from cord-blood were transduced at day 5 of the amplification step with the lentiviral vector pTRIPDU3/GFP expressing a shRNA targeting *RINF* mRNA expression (*shRNA/RINF*) or a non-target sequence (*shRNA/Control*). GFP<sup>+</sup> cells were sorted by fluorescent activated cell sorting 2 days after transduction. At that time, cell culture kinetics with less than 80% of CD36<sup>+</sup> cells or more than 5% of cell death (trypan blue) were not pursued. Erythropoietin (EPO) was added after sorting and maintained for 17–18 days. (B) *RINF* knockdown efficiency was estimated at the mRNA level by quantitative reverse transcriptase polymerase chain reaction (qRT-PCR) at DO of EPO (i.e., right after GFP-sorting). Here, the results are shown for one representative experiment out of seven independent experiments performed. A Student *t*-test was performed. (C) *RINF* knockdown efficiency was estimated at the protein level (specific band at 33 kDa) by western-blot analysis (see Methods). P85 (PIK3R1) was used as the loading control.<sup>42</sup> In order to obtain enough protein material, CD34<sup>+</sup> cells were amplified from a pool of five cord-blood units (5 donors). For each lane, protein extracted from 3x10<sup>6</sup> cells was loaded right after sorting, at DO of EPO. Band intensities were quantified with Multigauge software and the relative expression of *RINF* protein (normalized to the loading control) is indicated above the image in percentages of the *shControl* condition (D) Cell viability was assessed by the trypan blue exclusion method at 2 or 3 days after GFP-sorting. The histogram represents the percentage of trypan blue negative cells. (E) Cell culture growth was monitored in six independent experiments (here, cord-blood donors). The proliferation curve, expressed in cumulative population doublings, is shown for one representative experiment (donor#6, left panel). For most experiments (or “donors”), CD34<sup>+</sup> cells from several cord blood units (2–4) were pooled. Fold cell expansion (right panel) was calculated by dividing the absolute output number of expanded red blood cells after 17–18 days of culture with EPO by the respective number on day 0 (of treatment with EPO). An average reduction of ~45% was noted in the *RINF* knockdown condition (paired *t*-test, *P*=0.04, *n*=6). For two out of the six donors (donors 1 and 2, in gray), the *shRNA-RINF#4*-induced reduction in the total number of RBC was not obvious in our serum-free conditions (and absence of transforming growth factor β [TGFβ]). These two unresponsive donors were also treated with TGFβ, and data are presented in Figure 4E, F (F) Photographs of the five larger BFU-E colonies for the two conditions, here for one representative donor at day 11 (left panel). Two days after transduction (day 5 of expansion), GFP-expressing cells were sorted by flow cytometry and 500 cells per well were seeded into methylcellulose containing cytokines (IL3, SCF, G-CSF, GM-CSF, and EPO) enabling the formation of erythroid colonies (BFU-E). BFU-E colonies were imaged between 11 and 14 days of culture numerated from three donors (*n*=103 and *n*=110, respectively). The size of each BFU-E colony was determined by imaging analysis using ImageJ/Fiji. On average, the colonies were smaller for the *shRINF#4*-transduced condition (unpaired two-tailed *t*-test, *P*<0.01). (G) CD34<sup>+</sup> cells were isolated from bone marrow of healthy donors (*n*=4). Colony-forming cells (CFC) were counted between 11 and 14 days of culture. The histogram illustrates the mean number of small and large BFU-E-derived colonies. The error bars indicate donor-to-donor variability for each vector (± standard error of mean). To assess the effect of shRNA-mediated *RINF* silencing, a paired comparison was performed using the Fisher exact test.

TGFβ signaling pathway during *RINF* knockdown-dependent acceleration of erythropoiesis, we performed liquid cell culture experiments of primary CD34<sup>+</sup> cells in the presence of SB431542, a potent and selective inhibitor of TGFβRI<sup>35</sup> (Figure 4B). Strikingly, in the presence of SB431542, the maturation of *RINF* knockdown cells (evidenced by a faster acquisition of erythroid cell surface markers such as CD49d/Band3 at day 10 of EPO) was not accelerated and SMAD2 protein was not phosphorylated/activated after 3 days of EPO (Figure 4C, lanes 5 and 6), supporting the efficiency of the inhibitor. Conversely, in the absence of inhibitor, *RINF*-silencing gave rise to a faster rate of phosphorylation of SMAD2 protein, here noted at 8 h of EPO (Figure 4C compare lanes 1 and 2, or the kinetics of pSMAD2 waves in both conditions, right panel), indicating a higher sensitivity to autocrine TGFβ signaling, which would be mediated through SMAD2, as previously reported in hematopoietic cells.<sup>35</sup> A weaker RBC expansion was also noted for *RINF* knockdown cells, even when TGFβ1 (5 ng/mL) was added as late as day 11 of EPO treatment (Figure 4D). Moreover, even for the two donors whose *RINF* silencing was more subtle (donors 1 and 2, Figure 2E), *RINF* knockdown cells were more sensitive than control cells to TGFβ1 (Figure 4E, F). This was especially pronounced at low doses (0.1 ng/mL), at which we found faster acquisition of GPA (at day 6 of EPO) and reduced RBC production (at day 17 of EPO) (Figure 4F). Taken together, these data suggest that *RINF* knockdown cells were more sensitive to TGFβ and that the level of *RINF* in erythroid progenitors influences the upcoming RBC production, at least in the presence of TGFβ.

### Identification of SMAD7 as a *RINF* target gene candidate

To identify molecular mechanisms by which *RINF* might modulate responsiveness to TGFβ, we reanalyzed our previously published gene expression microarray datasets of K562 and UT7<sub>ss</sub> cells transduced with *shRINF#4* or *shControl*.<sup>7</sup> A relatively discrete set of 193 gene candidates (Online Supplementary Table S1) were downregulated by *RINF* knockdown in both cell lines. Strikingly, ingenuity pathway analyses revealed that this gene list was enriched in genes belonging to the TGFβ signaling pathway (Online Supplementary Figure S4C). Considering its well-known

inhibitory function on TGFβ-signaling and its low expression in MDS, *SMAD7* appeared as a promising candidate for functional investigation.<sup>33,34</sup> Encouragingly, *SMAD7* was also downregulated by *RINF* knockdown in a third hematopoietic cell line, MV4-11 (Online Supplementary Figure S4E, right panel) and the downregulation of *SMAD7* was confirmed by qRT-PCR analyses in K562 cells, even though the knockdown appeared moderate (~45%, *P*<0.001) in these independent experiments (Online Supplementary Figure S4D, right panel).

We next measured *RINF* levels in two cell line models of erythroid maturation, the K562 cell line treated with hemin and the UT7<sub>ss</sub> cell line treated with EPO<sup>39</sup> after GM-CSF withdrawal (Online Supplementary Figure S4A, B). In agreement with our findings in primary cells, *RINF* protein expression was downregulated upon treatment-induced erythroid differentiation, as early as 10 h after treatment with hemin for K562 cells, and after 2 days with EPO for UT7<sub>ss</sub> cells (Online Supplementary Figure S4A). Moreover, *RINF* knockdown accelerated the erythroid maturation program (Online Supplementary Figure S4B) triggered by hemin in K562 cells (noted after 1 day of treatment), or EPO in UT7<sub>ss</sub> cells (at 4 days of treatment). We also investigated whether *RINF* overexpression could delay hemoglobinization. To this end, we used the retroviral system MigR/IRES-GFP vector<sup>1</sup> (Online Supplementary Figure S5A, upper panel) to drive ectopic expression from full-length *RINF* cDNA. We found high constitutive expression of *RINF* protein for both cell lines (Online Supplementary Figure S5A), without cell toxicity or consequences on cell proliferation (not shown). When we evaluated erythroid differentiation using benzidine staining (Online Supplementary Figure S5B) we found that *RINF* overexpression reduced hemoglobinization in both cell lines (*P*<0.001), consistent with our knockdown experiments (Online Supplementary Figure S4A, B).

### *RINF* controls SMAD7 transcription directly

Our qRT-PCR analyses demonstrated a robust increase (approximately 5-fold) of *SMAD7* mRNA levels in cells overexpressing *RINF* (Figure 5A). To investigate whether *RINF*-mediated induction of *SMAD7* mRNA was direct and occurred at the transcriptional level, we performed ChIP experiments with anti-*RINF* antibodies. To this end, five sets of primers were designed for regions encompassing the

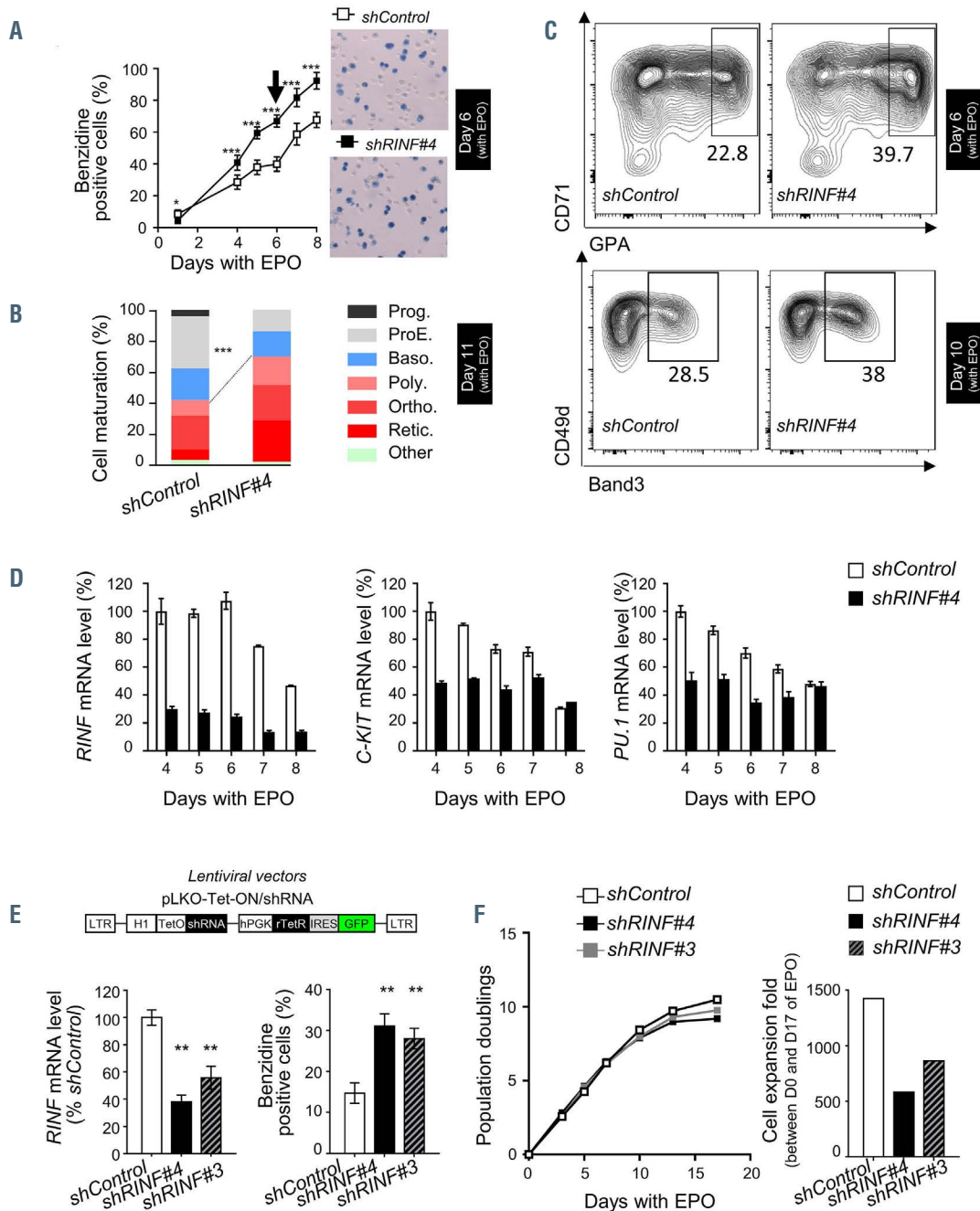


**Figure 3. RINF silencing accelerates erythroid maturation of human primary erythroblasts.** Erythroid differentiation was monitored in six separate experiments performed with CD34<sup>+</sup> cells isolated from either cord blood (n=3) or adult bone marrow (n=3), using different techniques. Despite donor-to-donor variability in the maturation kinetics, we consistently observed accelerated maturation for RINF knockdown conditions. Of note, data presented in Figure 3B, C correspond to two distinct donors. (A) Hemoglobin production of primary cells was estimated by a benzidine assay. CD34<sup>+</sup> cells isolated from cord blood were transduced with the lentiviral vector pTRIPDU3/GFP expressing a shRNA targeting RINF mRNA expression (shRNA/RINF) or a non-target sequence (shRNA/Control). GFP<sup>+</sup> cells were sorted by fluorescent activated cell sorting (FACS) 2 days after transduction. The black arrow at day 6 indicates the kinetic point selected for one representative picture in the right panel. (B) Morphological analysis was performed after staining with May-Grünwald-Giemsa (MGG). A Fisher exact test was applied to determine whether the observed acceleration of maturation was statistically significant. For this, enumerated erythroid cells (n=454) were segregated into either early (Progenitors, ProE, Baso) or late (Polychro, Ortho, Retic) groups. *P*<0.0001. (C) Erythroid maturation was also monitored by flow cytometry using anti-CD71 and anti-glycophorin-A (GPA/CD235a) labeled antibodies (upper panel) or using anti-CD49d and anti-Band3 antibodies (lower panel). Scattergrams of two representative experiments are shown (n=6), indicating a more mature population of cells for shRNA-RINF conditions either at day 6 of EPO (GPA<sup>+</sup>, upper panel), or at day 10 of EPO (Band3<sup>+</sup>, lower panel). (D) RINF loss of expression in human CD34<sup>+</sup> cells is also associated with accelerated downregulation of cKIT and PU.1. A histogram of relative mRNA expression determined by quantitative reverse transcriptase polymerase chain reaction (qRT-PCR) for RINF (left panel), cKIT (middle panel) and PU.1 (right panel). PU.1 and c-KIT mRNA are known to be downregulated upon erythroid maturation and are used here as molecular markers. In RINF knockdown cells (black bars), the downregulation of c-KIT and PU.1 mRNA preceded that observed in control cells by at least 3 days, in agreement with an accelerated maturation. (E, F) In order to validate our data with a second shRNA sequence targeting RINF, CD34<sup>+</sup> cells were transduced with the lentiviral vector pLKO-Tet-ON/shRNA vector, allowing doxycycline-inducible expression of shRNA sequences targeting RINF expression (shRINF#3 or shRINF#4). GFP<sup>+</sup> cells were sorted by FACS 2 days after transduction and cultured in the presence of doxycycline 0.2 µg/mL. (E) The left histogram represents the levels of RINF mRNA obtained with the two sequences targeting RINF (shRINF#3 or shRINF#4) and detected by qRT-PCR. Values are expressed in percentage of the shControl condition. The right histogram represents the percentages of benzidine positive cells obtained with the three shRNA sequences (shControl, shRINF#3, or shRINF#4). (F) Cell culture growth was monitored in one additional experiment (here, a pool from 2 adult donors) and the cumulative population doublings is indicated (left panel) as well as the fold expansion between D0 and D17 of treatment with erythropoietin (EPO) (right panel).

SMAD7 promoter (Figure 5B). As shown in *Online Supplementary Figure S5C*, we found that RINF binds directly to several regions (R1 to R4) of the SMAD7 promoter and that this binding was increased in cells overexpressing RINF. Moreover, H3K4me3 histone marks, quantified by

ChIP-qPCR (Figure 5C), were increased by RINF overexpression in four proximal regions (R2-R4) of the SMAD7 transcription start site, indicating that chromatin was in a more active transcriptional state.

To investigate functional relationships between RINF

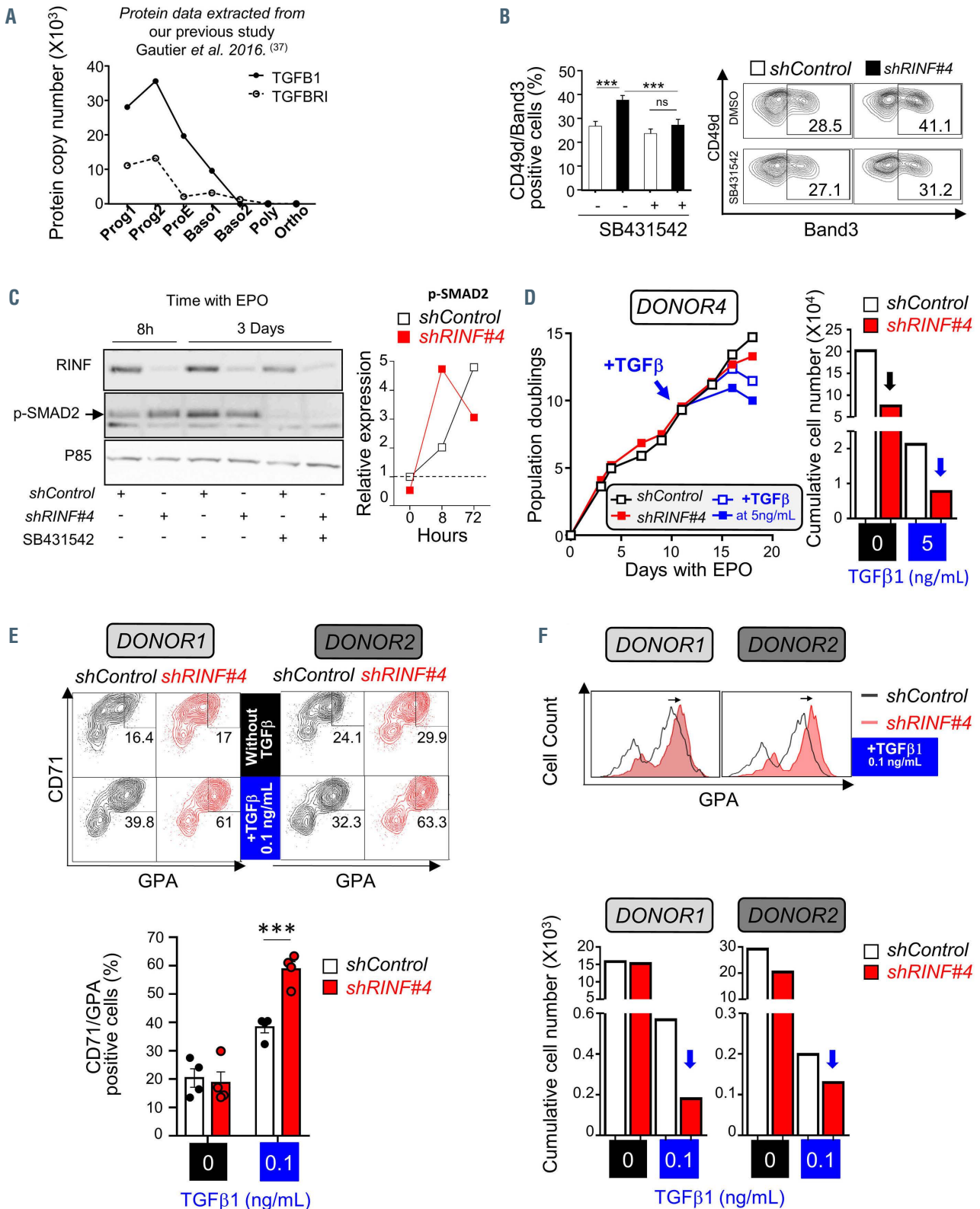


Figure 4. Legend on following page.

**Figure 4.** The *RINF* knockdown-induced phenotype is dependent on transforming growth factor  $\beta$  in human primary cells. (A) Transforming growth factor  $\beta$  (TGF $\beta$ ) ligand and TGFBR1 expression profiles were extracted from our proteomic analyses of cord blood-derived CD34<sup>+</sup> cells (Gauthier et al.<sup>37</sup>). TGF $\beta$ 1 and TGFBR1 were highly expressed at the Prog1-Prog2 stage (i.e. D1-D3 of erythropoietin [EPO] treatment), suggesting important autocrine signaling in early steps of erythroid maturation in our serum-free culture conditions. (B) Cord blood-derived CD34<sup>+</sup> cells were transduced at day 5 of the amplification step, GFP-sorted (2 days after transduction), and EPO was added for 8 to 12 days, in the presence of TGF $\beta$  inhibitor (SB431542, at 10  $\mu$ M) or vehicle control (dimethylsulfoxide, DMSO). The histograms (left panel) represents fluorescence activated cell sorting (FACS) analyses of the whole cell suspension for CD49d and Band3 antigens (here at 10 days of EPO). In order to determine whether the observed acceleration of maturation was statistically significant, Student *t*-tests were performed. Scattergrams (right panel) present one representative experiment out of three separate experiments performed. (C) *RINF* (left panel) and phosphorylated SMAD2 (right panel) protein levels were estimated at 8 h and 72 h of treatment with EPO by western-blot analysis (see Methods), with the same kinetics as presented in Figure 2C (pool of 5 cord blood units). As expected, the specific band for phospho-SMAD2 (Ser465/467), indicated by an arrow, was not detected in the presence of TGF $\beta$  inhibitor (SB431542, at 10  $\mu$ M). P85 (PIK3R1) was used as a loading control (lower panel) from the same blot, and at a shorter exposure time than in Figure 2C.<sup>42</sup> For each lane, protein extracted from 3x10<sup>6</sup> cells was loaded. Band intensities were quantified with Multigauge software and the relative phospho-SMAD2 expression is shown (right panel). (D) TGF $\beta$  (5 ng/mL) or vehicle control (DMSO) was added at 11 days of EPO and the proliferation monitored during 1 additional week, until day 18 of EPO. For both treated (in red) and untreated (in black) conditions, red blood cell expansion was lower for *RINF*-silenced cells. The kinetics shown corresponds to Donor#4 of Figure 2E (right panel). Cell culture growth is represented in population doublings (left panel) or cumulative cell number at day 18 of EPO (right panel). (E and F) The two donors (1 and 2) that seemed not sensitive to *RINF* knockdown in the absence of TGF $\beta$  (Figure 2E) were treated with variable doses of TGF $\beta$ 1 (ranging from 0.1 to 2.5 ng/mL), and scattergrams (upper panel) represent FACS analyses of the whole cell suspension labeled for both GPA and CD71 antigens. The corresponding dose-effect curves are also shown (lower panel). One representative scattergram at the lowest concentration (0.1 ng/mL) of exogenous TGF $\beta$ 1 is shown. (F) A histogram representing GPA acquisition (upper panel) which is more advanced in *RINF* knockdown cells (here at day 6 of EPO) in the presence of low doses of TGF $\beta$ 1 (here at 0.1 ng/mL). Cell growth was also monitored, and the total number of red blood cells numerated at day 17 of EPO are presented in the histograms (lower panel).

and *SMAD7*, we next performed “rescue” experiments in K562 cells. We employed retroviral transduction to express *SMAD7* ectopically (Figure 5D). Our data demonstrated that *SMAD7* overexpression did not affect endogenous expression of *RINF* mRNA or protein (Figure 5E, F), but did reduce hemoglobinization (Figure 5G, lane 3), mimicking the effect of ectopic *RINF* (Online Supplementary Figure S5B). We did not detect any change in cell viability or proliferation in the absence of hemin. Importantly, under conditions in which *SMAD7* was ectopically expressed, *RINF* knockdown did not result in acceleration of hemoglobinization (Figure 5G). Taken together, these data indicate that *RINF* binds the *SMAD7* promoter directly to control its expression, and that *SMAD7* is an effector downstream of *RINF* during erythroid maturation.

#### ***RINF* and *SMAD7* mRNA expression are correlated in bone marrow from adult donors and patients with myelodysplastic syndrome**

We investigated whether *RINF* and *SMAD7* mRNA expression correlated in primary human CD34<sup>+</sup> cells from healthy donors and donors with MDS. To this end, we performed qRT-PCR on CD34<sup>+</sup> cells isolated from adult bone marrow donors (n=11) and found a highly significant correlation between *RINF* mRNA and *SMAD7* mRNA (Pearson, rho=0.684, *P*=0.02) (Figure 6A). We confirmed these data by analyzing an independent microarray dataset from Pellagatti et al.<sup>46</sup> As shown in Figure 6B, *RINF* and *SMAD7* mRNA levels correlated strongly in CD34<sup>+</sup> cells isolated from healthy donors (Pearson rho=0.784, *P*<0.001, n=17). Interestingly, this correlation also reached statistical significance in CD34<sup>+</sup> cells from MDS -5q patients (Pearson rho=0.603, *P*<0.001, n=47) but not in other MDS patients, i.e., without del(5q) or 5q-. We then compared the intensity of this correlation with the other 5q genes (n=48 genes) from the commonly deleted regions associated with high risk, and the *CXXC5* probe sets were those correlating best with the *SMAD7* probe set in both the healthy control group (rho=0.819, and rho=0.784) and the MDS patients' cohort with del(5q) (Table 1) (Online Supplementary Figure S6A). Reinforcing the previously reported relevance of *SMAD7* in MDS pathophysiology,<sup>33,34</sup> *SMAD7* expression was not only extinguished in CD34<sup>+</sup> MDS samples compared to normal samples (in the microarray dataset from Gerstung et al.,<sup>47</sup> (Online Supplementary Figure S6C), but patients

with the lowest *SMAD7* expression had a significantly shorter overall survival (Online Supplementary Figure S6D).

#### ***RINF*-silencing alters genome-wide hydroxymethylation**

Since murine *RINF* has recently been described as a necessary platform for TET2 activity,<sup>15,48</sup> we wondered whether *RINF*-silencing could affect the genome-wide 5hmC of human immature erythroid cells. As shown in Figure 6C, we observed a statistically significant loss of 5hmC detected by immunofluorescence or flow cytometry (Figure 6D) in knockdown primary cells.

#### **A *RINF*/*SMAD7* axis controls erythroid maturation and red blood cell expansion in primary cells**

We next investigated whether *RINF* knockdown altered *SMAD7* expression in primary erythroid progenitors. As shown in Figure 7A, B, a 60-70% knockdown of *RINF* led to a statistically significant knockdown of *SMAD7* (by 40-45%) in CD34<sup>+</sup> cells isolated from cord blood (n=3 donors, paired Student *t*-test, *P*<0.001). Accordingly, a 30% knockdown of *SMAD7* protein level was detected by immunofluorescence in primary erythroid progenitors (*P*<0.0001) (Figure 7C). For a direct demonstration of the relevance of this finely tuned regulation of *SMAD7* mediated by *RINF* protein in primary HSPC, we next performed experiments in which we knocked down *RINF* and induced *SMAD7* expression ectopically. To this end, we first transduced CD34<sup>+</sup> cells with the doxycycline-inducible vector pInducer21/*SMAD7*-HA (Figure 7D), and then with the pTRIPUD3 vector that drives *shRNA/RINF* or *shRNA/Control* expression. Notably, in the presence of doxycycline, *SMAD7* expression (Figure 7E, F) robustly prevented both the *RINF* knockdown-dependent accelerated maturation (Figure 7G) and reduction of RBC numbers (Figure 7H).

#### **Discussion**

An increasing body of work suggests that *RINF* is involved in the maturation, function, or development of various cell types such as neural stem cells,<sup>21</sup> endothelial cells,<sup>49</sup> myoblasts,<sup>14</sup> myofibroblasts,<sup>24</sup> osteoblasts,<sup>23</sup> as well as in kidney development,<sup>22</sup> wound healing,<sup>24</sup> and hair regrowth.<sup>50</sup> Here, we report that the epigenetic factor *RINF* is a transcriptional regulator of *SMAD7* which fine-tunes TGF $\beta$  sensitivity of erythroid progenitors, findings that

bring insight into molecular barriers that may prevent effective erythropoiesis.

Our *in vitro* erythropoiesis experiments demonstrated that *RINF* is expressed in human erythroid progenitors (i.e., BFU-E and CFU-E) and proerythroblasts (ProE) but not in

the last stages. Loss of RINF expression does not affect cell viability or cell proliferation but accelerates erythroid maturation, and noticeably reduces RBC expansion. The average reduction in RBC number was estimated at ~45% in six experiments (Figure 2F) or one population doubling (i.e.,

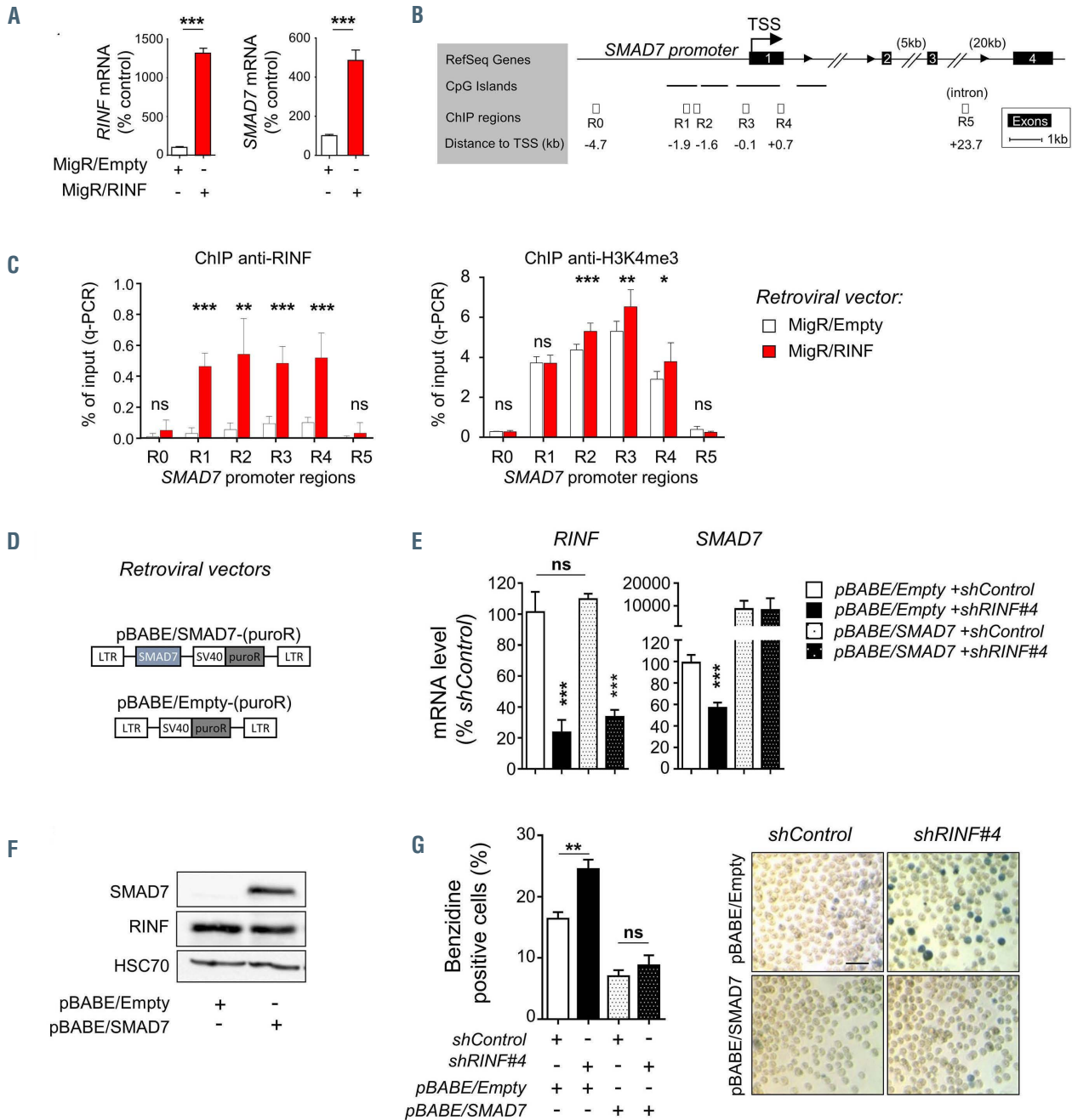


**Figure 5. SMAD7 is a direct transcriptional target of RINF.** (A) The MigR1 retroviral system was used to constitutively express RINF in the K562 cell line. A few days after transduction, cells were sorted for GFP expression and relative expression of *RINF* and *SMAD7* mRNA levels were measured by quantitative reverse transcriptase polymerase chain reaction (qRT-PCR). (B) Schematic representation of *SMAD7* gene structure (deduced from the ENCODE database). CpG islands and primer set regions (R0 to R5) used for chromatin immunoprecipitation (ChIP) experiments are also indicated as well as the distance to the transcription start site (TSS) of *SMAD7*. (C) ChIP-qPCR bars indicate the percentage of *SMAD7* promoter co-immunoprecipitated by anti-RINF (left panel) or anti-H3K4me3 (right panel) antibody in the K562 cell line. (D) Schematic representation of the pBABE retroviral vector used for *SMAD7* overexpression or empty cassette control. (E) Histograms representing the *RINF* and *SMAD7* mRNA levels detected by qRT-PCR. Values are expressed in percentage of the shControl condition. A Student *t*-test (unpaired) was performed to assess whether relative expression values were statistically significant from those of the shControl condition. (F) Relative expression of RINF and SMAD7 was measured by western-blot analysis after retroviral transduction of K562 cells with pBABE/SMAD7 or pBABE/Empty and puromycin selection (1  $\mu$ g/mL) for 5 days. HSC70 was used as a loading control. (G) K562/SMAD7 and K562/Empty cells were then transduced with pTRIPDU3 lentiviral vector. Cells were sorted for GFP expression 2 days after transduction. To analyze hemoglobin production, the benzidine test was used after 24 h of exposure to hemin. The percentage of benzidine-positive cells was established by counting at least 300 cells per sample. Pictures represent one of three independent experiments. For statistical analysis a Student *t*-test was performed for qPCR experiments, and hemoglobin production analysis (\*\* $P=0.0026$ ; ns:  $P>0.05$ ).

1.03, for the 4 donors #3-6), suggesting that RINF knock-down cells could skip one division (in the presence of TGF $\beta$ ). Our data indicate that RINF-dependent erythroid maturation is also dependent on TGF $\beta$  signaling at physiological levels. This cytokine, a potent inducer of erythroid maturation and growth inhibition,<sup>27,29,51,52</sup> is known to be enriched in the bone marrow microenvironment<sup>53</sup> and we surmise that the RINF/SMAD7 regulation axis that we describe here is likely to exert a more pronounced effect *in vivo* than in our serum-free culture conditions (i.e., without exogenous TGF $\beta$ ). Moreover, since the mechanism of action is SMAD7-dependent, RINF downregulation may also sensitize hematopoietic cells to other cytokines of the TGF $\beta$  superfamily which may act on late-stage erythropoiesis *in vivo* (such as activins and GDF11).<sup>54-57</sup> In this manner, RINF could be one of the players regulating the dynam-

ic balance between long-term expansion of the erythroid pool *versus* fast production of RBC for immediate physiological needs.

Two recent studies suggest that murine RINF could act as an anchoring platform necessary for TET2 (which lacks a CXXC domain) and its activity at CpG sites (5'-hydroxymethylation), in plasmacytoid dendritic cells<sup>15</sup> and mouse embryonic stem cells.<sup>48</sup> Conversely, an earlier study indicated that RINF inhibits TET2 and hydroxymethylation of genomic DNA in a caspase-dependent manner (in mouse embryonic stem cells), and another one indicated that RINF binds to unmethylated (and not methylated) CpG sites,<sup>18</sup> probably reflecting a more complex mechanism of action.<sup>12</sup> We here provide the first experimental evidence (to our knowledge) that RINF can regulate genome-wide hydroxymethylation in human

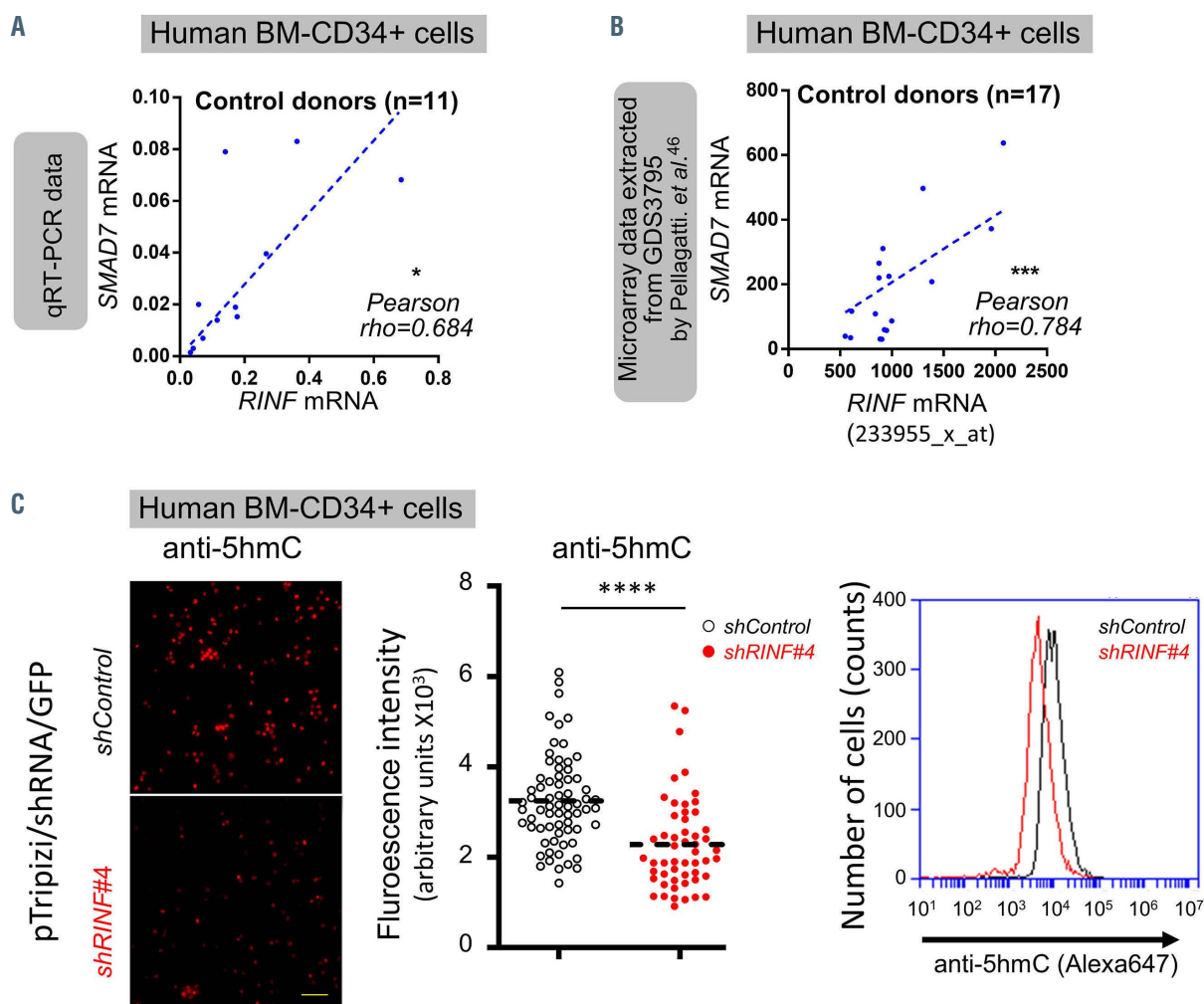


**Figure 6.** RINF and SMAD7 mRNA closely correlate in primary human CD34<sup>+</sup> bone marrow cells isolated from healthy donors or myelodysplastic syndrome patients with del(5q) and RINF-silencing leads to global loss of 5-hydroxymethylation. (A) CD34<sup>+</sup> cells were isolated from adult bone marrow (n=11). RINF and SMAD7 mRNA levels were measured by quantitative reverse transcriptase polymerase chain reaction (qRT-PCR). In order to assess whether the expression of these two genes correlated in donors' samples, a correlation analysis was performed with the Pearson correlation coefficient method (for non-parametric analysis): rho=0.684, P(two-tailed) <0.05 (B) RINF and SMAD7 gene expression data were extracted from a previously described microarray dataset published by Pellagatti et al.<sup>46</sup> In this study, CD34<sup>+</sup> cells were isolated from adult bone marrow (n=17). For mRNA detection, the 233955\_x\_at and 204790\_at probesets were used for CXXC5 and SMAD7, respectively. A correlation analysis was performed with the Pearson rho (for non-parametric analysis). Strong correlation coefficients were noted for normal healthy controls (rho=0.784) and myelodysplastic syndrome (MDS) patients with del(5q), (rho=0.603), which were both highly significant: P(two-tailed) <0.001. (C) CD34<sup>+</sup> cells isolated from cord blood or healthy adult donors were transduced with pTripizi vector expressing a shRNA targeting RINF expression (shRNA/RINF#4) or a "non-target" shRNA (shRNA/Control). A couple of days later, during the amplification phase (see Figure 1A), cells were GFP-sorted and 5hmC was detected by immunofluorescence (left panel) or flow cytometry (right panel) using an anti-5hmC antibody labeled with a fluorescent dye. The intensity of the labeling was also quantified by cell imaging analysis using Fiji software. Representative images from three independent experiments are shown. Here, the CD34<sup>+</sup> cells are from an adult donor at 4 days of expansion (2 days after transduction). Scale bar=50  $\mu$ m.

**Table 1.** List of genes located at 5q and their correlation with SMAD7 expression in primary human CD34<sup>+</sup> cells isolated from bone marrow of healthy donors (n=17).

Gene name	Probeset	Pearson's (correl coeff.)	Gene location at 5q
CXXC5	222996_s_at	0.819	High-Risk CDR
CXXC5	233955_x_at	0.784	High-Risk CDR
HSPA9	200690_at	0.729	High-Risk CDR
CXXC5	224516_s_at	0.705	High-Risk CDR
ETF1	201574_at	0.640	High-Risk CDR
IL17B	220273_at	0.554	Low-Risk CDR
SPARC	212667_at	0.532	Low-Risk CDR
ETF1	201573_s_at	0.508	High-Risk CDR
MATR3	238993_at	0.452	High-Risk CDR
CD74	1567627_at	0.424	Low-Risk CDR
TGFB1	201506_at	0.422	High-Risk CDR
PDGFRB	202273_at	0.391	Low-Risk CDR
EGR1	201694_s_at	0.373	High-Risk CDR
SIL1	218436_at	0.355	High-Risk CDR
PSD2	223536_at	0.352	High-Risk CDR
UBE2D2	201345_s_at	0.350	High-Risk CDR
AFAP1L1	155542_at	0.343	Low-Risk CDR
SH3TC2	233561_at	0.337	Low-Risk CDR
CSF1R	203104_at	0.335	Low-Risk CDR
TMEM173	224916_at	0.312	High-Risk CDR
PAIP2	222983_s_at	0.289	High-Risk CDR
HNRNPA0	229083_at	0.271	High-Risk CDR
CDX1	206430_at	0.259	Low-Risk CDR
EGR1	201693_s_at	0.214	High-Risk CDR
FAM53C	218023_s_at	0.193	High-Risk CDR
AFAP1L1	226955_at	0.184	Low-Risk CDR
MZB1	223565_at	0.180	High-Risk CDR
CARMN	231987_at	0.180	Low-Risk CDR
CDC23	223651_x_at	0.178	High-Risk CDR
CTNNA1	200764_s_at	0.176	High-Risk CDR
REEP2	205331_s_at	0.167	High-Risk CDR
SPATA24	238027_at	0.137	High-Risk CDR
RPS14	208645_s_at	0.134	Low-Risk CDR
LRRTM2	206408_at	0.128	High-Risk CDR

continued in the next column

continued from the previous column

NRG2	242303_at	0.122	High-Risk CDR
GFRA3	229936_at	0.114	High-Risk CDR
BRD8	242265_at	0.096	High-Risk CDR
CDC25C	216914_at	0.083	High-Risk CDR
SH3TC2	240966_at	0.052	Low-Risk CDR
HNRNPA0	201055_s_at	0.041	High-Risk CDR
KDM3B	210878_s_at	0.041	High-Risk CDR
GRPEL2	238427_at	0.040	Low-Risk CDR
TMEM173	224929_at	0.028	High-Risk CDR
EGR1	227404_s_at	0.013	High-Risk CDR
DNAJC18	227166_at	-0.018	High-Risk CDR
FAM13B	218518_at	-0.025	High-Risk CDR
TRPC7	208589_at	-0.035	High-Risk CDR
ABLIM3	205730_s_at	-0.068	Low-Risk CDR
NME5	206197_at	-0.081	High-Risk CDR
KLHL3	1555110_a_at	-0.094	High-Risk CDR
WNT8A	224259_at	-0.116	High-Risk CDR
SPATA24	1558641_at	-0.137	High-Risk CDR
LECT2	207409_at	-0.143	High-Risk CDR
IL9	208193_at	-0.157	High-Risk CDR
ECSCR	227780_s_at	-0.169	High-Risk CDR
KLHL3	221221_s_at	-0.179	High-Risk CDR
PKD2L2	221118_at	-0.187	High-Risk CDR
ZNF300	228144_at	-0.191	Low-Risk CDR
SMAD5	225223_at	-0.221	High-Risk CDR
TRPC7	202363_at	-0.241	High-Risk CDR
SH3TC2	219710_at	-0.315	Low-Risk CDR
SLC23A1	223732_at	-0.319	High-Risk CDR
CDC25C	205167_s_at	-0.351	High-Risk CDR
MYOT	219728_at	-0.386	High-Risk CDR
UBE2D2	201344_at	-0.538	High-Risk CDR
PCYOX1L	218953_s_at	-0.559	Low-Risk CDR
GRPEL2	226881_at	-0.614	Low-Risk CDR
KIF20A	218755_at	-0.786	High-Risk CDR

All the genes were selected because they are located within one of the two commonly deleted regions (CDR) at chromosome 5q. Their mRNA expression level was extracted from a GDS3795 microarray study performed by Pellagatti *et al.*<sup>16</sup> For each gene, a Pearson correlation coefficient was calculated by comparing its expression to the one of SMAD7, and the list is ranked by descending order.

cells. The role of RINF that we describe here could pave the way to future studies that will be necessary to better understand the complex molecular epigenetic events that occur during normal and ineffective erythropoiesis<sup>12,15,48,58</sup> and that may involve TET enzymes.<sup>59</sup>

Several correlative studies have implicated RINF as a candidate in the pathogenesis of MDS/AML.<sup>1,3,5,60</sup> MDS is a complex and heterogeneous malignant hematologic disorder in which the loss of several genes is suspected to lead to the pathophysiology.<sup>4</sup> CXXC5 is located at chromosome 5q31.2, in a commonly deleted region associated with high risk in MDS and AML (Online Supplementary Figure S4).<sup>1,4</sup> Even though it is uncertain that RINF loss of expression in itself can cause the development of preleukemia, our functional data in human CD34<sup>+</sup> cells indicate that loss of RINF may exacerbate cytopenia of

the erythroid lineage. Of importance, the functional contribution of *Cxxc5/Rinf* loss of function to MDS development was recently described in a mouse model, in which its invalidation (by random insertional mutation) was demonstrated to cooperate with *Egr1* haploinsufficiency to promote MDS.<sup>4</sup> This study indicated that the *Cxxc5* gene could act as a tumor suppressor gene contributing to del(5q) myeloid neoplasms. Although RINF/CXXC5 is not frequently mutated in patients with MDS/AML,<sup>60</sup> several recurrent chromosomal anomalies or gene mutations could lead to RINF loss of expression and contribute in the long-term to ineffective erythropoiesis and/or myeloid transformation (legend of Online Supplementary Figure S7).

Our findings point to a molecular mechanism in which RINF functions as a negative modulator of TGFβ signaling

by upregulating and maintaining SMAD7. Consequently, *RINF* loss of expression will sensitize human erythroid progenitors to autocrine/paracrine TGF $\beta$ -induced growth inhibition as a mechanism to prevent expansion of the erythroid pool. Our data also suggest that this signaling would be at least partly mediated through SMAD2 activation and phosphorylation (Figure 4C), in agreement with a previous report on human bone marrow.<sup>35</sup> The *in*

*vivo* relevance of these findings is strengthened by the correlated *RINF* and *SMAD7* mRNA expression in human bone marrow CD34<sup>+</sup> cells. This correlation was also observed in MDS patients with del(5q) or 5q- but not in other forms of MDS, in which *SMAD7* was silenced in most of the patients' samples, whatever the *RINF* expression level. This extinction of *SMAD7* in other MDS could be explained by various mechanisms such as miRNA21

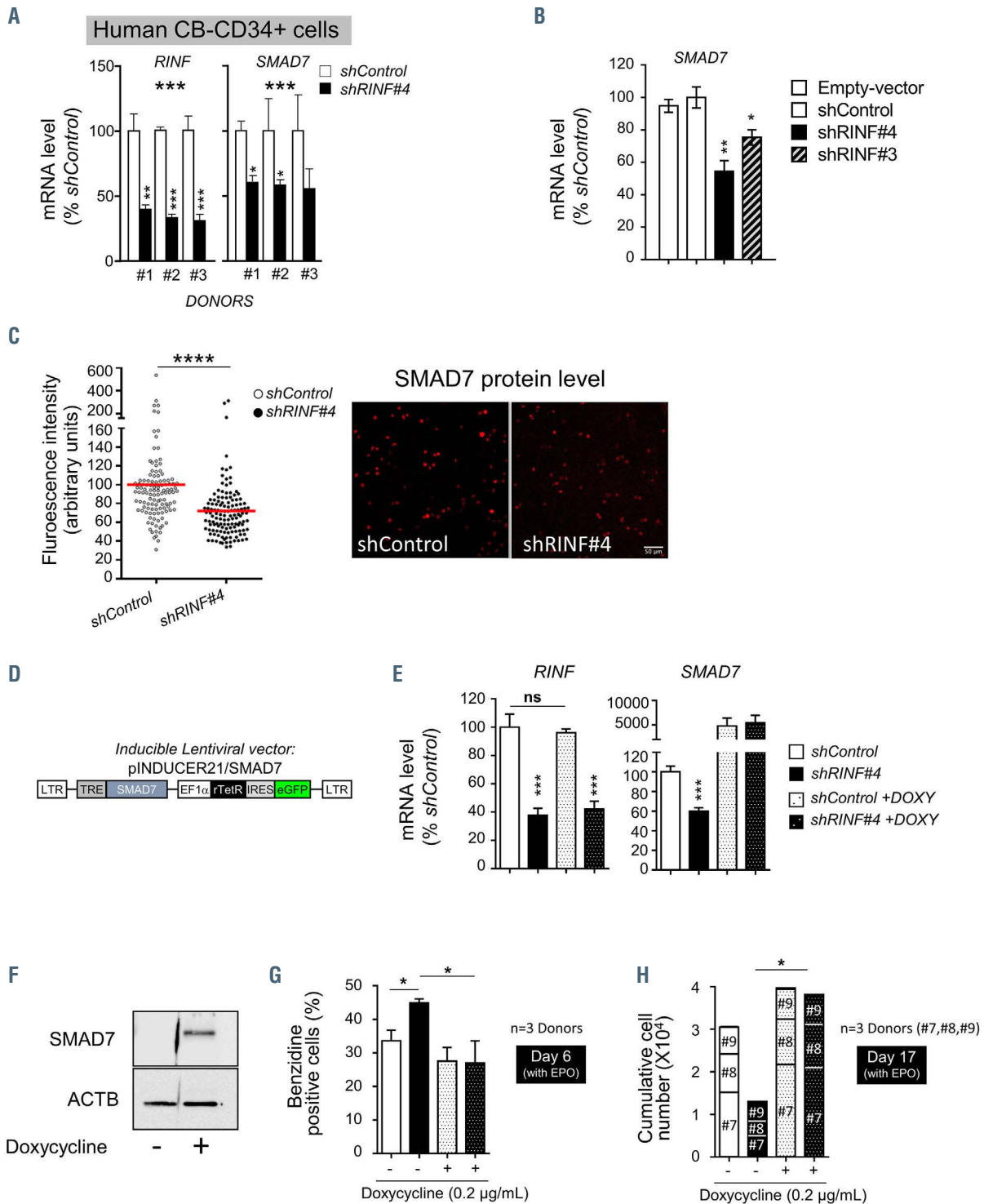


Figure 7. Legend on following page.

**Figure 7.** The *RINF* knockdown-induced phenotype is *SMAD7*-dependent in human primary cells. (A) Histogram representing *RINF* (left panel) and *SMAD7* (right panel) mRNA expression levels in shRNA-transduced CD34<sup>+</sup> cells isolated from three cord blood units. In these specific experiments, lentiviral transduction was performed after magnetic sorting of CD34<sup>+</sup> cells (i.e., day 0 of the amplification step) and cells were GFP-sorted between 2 and 5 days of the amplification step. Data shown are mean  $\pm$  standard deviation for each donor (the quantitative reverse transcriptase polymerase chain reaction [qRT-PCR] was performed in triplicate). To assess whether the mRNA level was statistically different between *shRNA-RINF* and *shRNA-Scramble* samples, a Student *t*-test was performed for each donor. Considering the three biological replicates, both *RINF* and *SMAD7* mRNA levels were statistically downregulated by *shRNA-RINF* (paired Student *t*-test,  $P < 0.001$ ). (B) This histogram represents the level of *SMAD7* mRNA obtained with the two sequences targeting *RINF* (*shRINF#3* and *shRINF#4*) and detected by qRT-PCR. Values are expressed as percentages of the shControl condition. *RINF* mRNA levels are shown in Online Supplementary Figure S3B. (C) Since detection of *SMAD7* protein level requires a large quantity of cells for western blot analysis and the active endogenous level of this protein can be below the detection threshold, *SMAD7* protein levels were estimated by immunofluorescence. Images of stained cells were acquired on a wide-field Nikon Eclipse microscope through a  $\times 20$  objective, with an Eclipse TE2000, a cascade CDD camera (Photometrics). Images of *SMAD7* had to be acquired with a binning of one, and two images were averaged for each condition. For cell imaging analysis the quantification of the labeling, performed on two images after background subtraction, the mean fluorescent intensity was measured in 100–120 cells for the two conditions, using Fiji software. Representative images from three independent experiments are shown. Scale bar = 50  $\mu$ m. (D) Schematic representation of the pInducer21/*SMAD7* lentiviral vector used for rescue experiments. This vector drives the expression of *SMAD7*/HA under a tetracycline response element (TRE) promoter that is activated after doxycycline treatment. To perform rescue experiments, cord blood-derived CD34<sup>+</sup> cells ( $n = 3$  donors) were first transduced with the pInducer21/*SMAD7* lentiviral vector, sorted for a low GFP expression, and transduced again with the pTRIPDU3/shRNA vectors targeting *RINF* or control. After a second step of GFP sorting (this time based on high GFP expression to sort cells transduced with both lentiviral vectors), cells were cultured for 2 more days before adding (or not) doxycycline, which induced *SMAD7* expression. (E) Histograms representing *RINF* and *SMAD7* mRNA levels in cells, detected by qRT-PCR. Values are expressed as percentages of the shControl condition. A Student *t*-test (unpaired) was performed to assess whether the observed relative difference was statistically significant. (F) *RINF* and *SMAD7* were detected by western-blot analysis after doxycycline induction (here after 3 days of treatment with 0.2  $\mu$ g/mL). ACTB was used as a loading control. (G) Cell maturation was determined by a benzidine assay (upper panel histogram). (H) Cumulative red blood cell number at day 17 of exposure to erythropoietin (EPO) is presented in the histogram in the lower panel.

expression.<sup>33</sup> However, since *RINF* knockdown leads to global loss of 5hmC, it is tempting to speculate that the loss of *RINF* could lead to hypermethylation of the *SMAD7* promoter in HSPC, a process that could have gone unnoticed in previous studies. Interestingly, the *SMAD7* promoter is known to be silenced by hypermethylation in non-hematopoietic tissues, and hypomethylating agents such as azacytidine can revert this hypermethylation, and alleviates TGF $\beta$ -induced diseases in several pathological models such as atherosclerosis,<sup>61</sup> renal fibrosis<sup>62</sup> and liver fibrosis.<sup>63</sup> Thus, further studies should investigate whether the *SMAD7* promoter is demethylated after treatment with hypomethylating agents (azacytidine or decitabine) in human HSPC isolated from MDS patients, and to what extent this mechanism could contribute to the efficacy of these epigenetic drugs to sustain erythropoiesis in the long-term. In support of this concept, *TET2* mutation is a good indicator of response to azacytidine treatment.<sup>64</sup>

Previous studies have underscored the importance of *SMAD7* regulation in MDS.<sup>33,34</sup> Our present data complement these studies by demonstrating, first, a direct transcriptional mechanism by which *SMAD7* is regulated in hematopoietic cells and, second, that the residual level of *SMAD7* in MDS is associated with the severity of the disease and patients' survival (Online Supplementary Figure S6D). These data are particularly relevant in the context of understanding how responsiveness to TGF $\beta$  in the bone marrow microenvironment is fine-tuned,<sup>28</sup> and in a context-specific manner.<sup>30</sup> Even though this mechanism is unlikely to be solely responsible for TGF $\beta$ -hypersensitivity, our findings pave the way for novel research avenues in blood disorders characterized by ineffective erythropoiesis such as myelofibrosis,<sup>65</sup> Fanconi anemia,<sup>66</sup>  $\beta$ -thalassemia,<sup>57,67</sup> and MDS,<sup>55</sup> and for which novel therapies based on TGF $\beta$  inhibitors are particularly promising.<sup>56,68</sup> Finally, beyond its role during erythropoiesis, the *RINF*/*SMAD7* regulation axis described here could, at least partly, contribute to the pleiotropic effects of *RINF* described during wound healing,<sup>24</sup> fibrosis,<sup>61–63,69</sup> immunity,<sup>15</sup> and tumor biology,<sup>1,3,6–9</sup> and deserves to be investigated in these physiological processes.

### Disclosures

FP is a holder of patents describing methods for *RINF* mRNA detection (WO2009/151337 and WO2012/010664). The other authors declare that they have no potential conflicts of interest.

### Contributions

AA and GM performed most of the experiments. DS and SZ performed the ChIP experiments. YZ, VF, IM, and E-FG performed some experiments and discussed the data. AA, GM, FV, EL, MF, AK, OD, and CL discussed the data. ES-B, ID-F, DB, OH, and PM supervised the study. FP conceived the study and supervised the experiments. AA, GM, and FP analyzed the data, created the figures and wrote the manuscript.

### Acknowledgments

The authors thank Pr. Jérôme Larghero and Thomas Domet from Centre de Ressources Biologiques / Banque de Sang de Cordon de l'AP-HP (Saint-Louis Hospital) for providing cord blood units, Anne Dubart-Kupperschmitt for the pTRIPDU3/GFP vector,<sup>40</sup> Johan Lillehaug, Øystein Bruserud, Camille Humbert, Pierre de la Grange (Genosplice), Eric Nguyen, Sabrina Bondu, Alexandre Artus, Amandine Houvert, Nadège Berovic, Emmanuel Donnadieu, Franck Letourneur, Brigitte Izac, Sebastien Jacques, and Alain Trautmann for technical assistance and scientific discussions, as well as Life Science Editors for reading and editing the manuscript. We are grateful to the staff of the IMAG'IC, CYBIO, and GENOM'IC facilities of the Cochin Institute.

### Funding

This work was supported by INSERM, Paris-Descartes University, the Ligue Nationale Contre le Cancer (LNCC), the Cochin Institute, and the Laboratory of Excellence GR-EX. AA was supported by LNCC, Société Française d'Hématologie, Fondation pour la Recherche Médicale, and Boehringer Society (travel grant). GM was supported by a fellowship grant from the Ministère de l'Enseignement Supérieur et de la Recherche and Société Française d'Hématologie. ES-B is supported by the National Center for Scientific Research (CNRS) and her team was supported by LNCC and Fondation de France. We are also grateful for support from the French-Norwegian exchange program (Aurora to FP).

## References

- Pendino F, Nguyen E, Jonassen I, et al. Functional involvement of RINF, retinoid-inducible nuclear factor (CXXC5), in normal and tumoral human myelopoiesis. *Blood*. 2009;113(14):3172-3181.
- Jerez A, Gondek LP, Jankowska AM, et al. Topography, clinical, and genomic correlates of 5q myeloid malignancies revisited. *J Clin Oncol*. 2012;30(12):1343-1349.
- Kuhnl A, Valk PJ, Sanders MA, et al. Downregulation of the Wnt inhibitor CXXC5 predicts a better prognosis in acute myeloid leukemia. *Blood*. 2015;125(19):2985-2994.
- Stoddart A, Qian Z, Fernald AA, et al. Retroviral insertional mutagenesis identifies the del(5q) genes, CXXC5, TIFAB and ETF1, as well as the Wnt pathway, as potential targets in del(5q) myeloid neoplasms. *Haematologica*. 2016;101(6):e232-236.
- Treppendahl MB, Mollgard L, Hellstrom-Lindberg E, Cloos P, Gronbaek K. Downregulation but lack of promoter hypermethylation or somatic mutations of the potential tumor suppressor CXXC5 in MDS and AML with deletion 5q. *Eur J Haematol*. 2013;90(3):259-260.
- Astori A, Fredly H, Aloysius TA, et al. CXXC5 (retinoid-inducible nuclear factor, RINF) is a potential therapeutic target in high-risk human acute myeloid leukemia. *Oncotarget*. 2013;4(9):1438-1448.
- Bruserud O, Reikvam H, Fredly H, et al. Expression of the potential therapeutic target CXXC5 in primary acute myeloid leukemia cells - high expression is associated with adverse prognosis as well as altered intracellular signaling and transcriptional regulation. *Oncotarget*. 2015;6(5):2794-2811.
- Benedetti I, De Marzo AM, Geliebter J, Reyes N. CXXC5 expression in prostate cancer: implications for cancer progression. *Int J Exp Pathol*. 2017;98(4):234-243.
- Knappskog S, Myklebust LM, Busch C, et al. RINF (CXXC5) is overexpressed in solid tumors and is an unfavorable prognostic factor in breast cancer. *Ann Oncol*. 2011;22(10):2208-2215.
- Zhang M, Wang R, Wang Y, et al. The CXXC finger 5 protein is required for DNA damage-induced p53 activation. *Sci China C Life Sci*. 2009;52(6):528-538.
- Aras S, Pak O, Sommer N, et al. Oxygen-dependent expression of cytochrome c oxidase subunit 4-2 gene expression is mediated by transcription factors RBPJ, CXXC5 and CHCHD2. *Nucleic Acids Res*. 2013;41(4):2255-2266.
- Ko M, An J, Bandukwala HS, et al. Modulation of TET2 expression and 5-methylcytosine oxidation by the CXXC domain protein IDAX. *Nature*. 2013;497(7447):122-126.
- L'Hote D, Georges A, Todeschini AL, et al. Discovery of novel protein partners of the transcription factor FOXL2 provides insights into its physiopathological roles. *Hum Mol Genet*. 2012;21(14):3264-3274.
- Li G, Ye X, Peng X, et al. CXXC5 regulates differentiation of C2C12 myoblasts into myocytes. *J Muscle Res Cell Motil*. 2014;35(5-6):259-265.
- Ma S, Wan X, Deng Z, et al. Epigenetic regulator CXXC5 recruits DNA demethylase Tet2 to regulate TLR7/9-elicited IFN response in pDCs. *J Exp Med*. 2017;214(5):1471-1491.
- Marshall PA, Hernandez Z, Kaneko I, et al. Discovery of novel vitamin D receptor interacting proteins that modulate 1,25-dihydroxyvitamin D3 signaling. *J Steroid Biochem Mol Biol*. 2012;132(1-2):147-159.
- Yasar P, Ayaz G, Muyan M. Estradiol-estrogen receptor alpha mediates the expression of the CXXC5 gene through the estrogen response element-dependent signaling pathway. *Sci Rep*. 2016;6:37808.
- Ayaz G, Razizadeh N, Yasar P, et al. CXXC5 as an unmethylated CpG dinucleotide binding protein contributes to estrogen-mediated cellular proliferation. *Sci Rep*. 2020;10(1):5971.
- Long HK, Blackledge NP, Klose RJ. ZF-CxxC domain-containing proteins, CpG islands and the chromatin connection. *Biochem Soc Trans*. 2013;41(3):727-740.
- Melamed P, Yosefzon Y, David C, Tsukerman A, Pnueli L. Tet enzymes, variants, and differential effects on function. *Front Cell Dev Biol*. 2018;6:22.
- Andersson T, Sodersten E, Duckworth JK, et al. CXXC5 is a novel BMP4-regulated modulator of Wnt signaling in neural stem cells. *J Biol Chem*. 2009;284(6):3672-3681.
- Kim MS, Yoon SK, Bollig F, et al. A novel Wilms tumor 1 (WT1) target gene negatively regulates the WNT signaling pathway. *J Biol Chem*. 2010;285(19):14585-14593.
- Kim HY, Yoon JY, Yun JH, et al. CXXC5 is a negative-feedback regulator of the Wnt/beta-catenin pathway involved in osteoblast differentiation. *Cell Death Differ*. 2015;22(6):912-920.
- Lee SH, Kim MY, Kim HY, et al. The Dishevelled-binding protein CXXC5 negatively regulates cutaneous wound healing. *J Exp Med*. 2015;212(7):1061-1080.
- Pardali K, Moustakas A. Actions of TGF-beta as tumor suppressor and pro-metastatic factor in human cancer. *Biochim Biophys Acta*. 2007;1775(1):21-62.
- Siegel PM, Massague J. Cytostatic and apoptotic actions of TGF-beta in homeostasis and cancer. *Nat Rev Cancer*. 2003;3(11):807-821.
- Zermati Y, Varet B, Hermine O. TGF-beta1 drives and accelerates erythroid differentiation in the epo-dependent UT-7 cell line even in the absence of erythropoietin. *Exp Hematol*. 2000;28(3):256-266.
- Blank U, Karlsson S. TGF-beta signaling in the control of hematopoietic stem cells. *Blood*. 2015;125(23):3542-3550.
- Krystal G, Lam V, Dragowska W, et al. Transforming growth factor beta 1 is an inducer of erythroid differentiation. *J Exp Med*. 1994;180(3):851-860.
- Ruscetti FW, Akel S, Bartelmez SH. Autocrine transforming growth factor-beta regulation of hematopoiesis: many outcomes that depend on the context. *Oncogene*. 2005;24(37):5751-5763.
- Derynck R, Zhang YE. Smad-dependent and Smad-independent pathways in TGF-beta family signalling. *Nature*. 2003;425(6958):577-584.
- Shi Y, Massague J. Mechanisms of TGF-beta signaling from cell membrane to the nucleus. *Cell*. 2003;113(6):685-700.
- Bhagat TD, Zhou L, Sokol L, et al. miR-21 mediates hematopoietic suppression in MDS by activating TGF-beta signaling. *Blood*. 2013;121(15):2875-2881.
- Zhou L, McMahon C, Bhagat T, et al. Reduced SMAD7 leads to overactivation of TGF-beta signaling in MDS that can be reversed by a specific inhibitor of TGF-beta receptor I kinase. *Cancer Res*. 2011;71(3):955-963.
- Zhou L, Nguyen AN, Sohal D, et al. Inhibition of the TGF-beta receptor I kinase promotes hematopoiesis in MDS. *Blood*. 2008;112(8):3434-3443.
- Freyssinier JM, Lecoq-Lafon C, Amsellem S, et al. Purification, amplification and characterization of a population of human erythroid progenitors. *Br J Haematol*. 1999;106(4):912-922.
- Gautier EF, Ducamp S, Leduc M, et al. Comprehensive proteomic analysis of human erythropoiesis. *Cell Rep*. 2016;16(5):1470-1484.
- Inman GJ, Nicolas FJ, Callahan JF, et al. SB-431542 is a potent and specific inhibitor of transforming growth factor-beta superfamily type I activin receptor-like kinase (ALK) receptors ALK4, ALK5, and ALK7. *Mol Pharmacol*. 2002;62(1):65-74.
- Millot GA, Vainchenker W, Dumenil D, Svinarchuk F. Differential signalling of NH2-terminal flag-labelled thrombopoietin receptor activated by TPO or anti-FLAG antibodies. *Cell Signal*. 2004;16(3):355-363.
- Amsellem S, Ravet E, Fichelson S, Pflumio F, Dubart-Kupperschmitt A. Maximal lentivirus-mediated gene transfer and sustained transgene expression in human hematopoietic primitive cells and their progeny. *Mol Ther*. 2002;6(5):673-677.
- Papageorgis P, Lambert AW, Ozturk S, et al. Smad signaling is required to maintain epigenetic silencing during breast cancer progression. *Cancer Res*. 2010;70(3):968-978.
- Lecoq-Lafon C, Verdier F, Fichelson S, et al. Erythropoietin induces the tyrosine phosphorylation of GAB1 and its association with SHC, SHP2, SHIP, and phosphatidylinositol 3-kinase. *Blood*. 1999;93(8):2578-2585.
- Merryweather-Clarke AT, Atzberger A, Soneji S, et al. Global gene expression analysis of human erythroid progenitors. *Blood*. 2011;117(13):e96-108.
- An X, Schulz VP, Li J, et al. Global transcriptome analyses of human and murine terminal erythroid differentiation. *Blood*. 2014;123(22):3466-3477.
- Keller MA, Addya S, Vadigepalli R, et al. Transcriptional regulatory network analysis of developing human erythroid progenitors reveals patterns of coregulation and potential transcriptional regulators. *Physiol Genomics*. 2006;28(1):114-128.
- Pellagatti A, Cazzola M, Giagounidis AA, et al. Gene expression profiles of CD34+ cells in myelodysplastic syndromes: involvement of interferon-stimulated genes and correlation to FAB subtype and karyotype. *Blood*. 2006;108(1):337-345.
- Gerstung M, Pellagatti A, Malcovati L, et al. Combining gene mutation with gene expression data improves outcome prediction in myelodysplastic syndromes. *Nat Commun*. 2015;6:5901.
- Ravichandran M, Lei R, Tang Q, et al. Rinf regulates pluripotency network genes and Tet enzymes in embryonic stem cells. *Cell Rep*. 2019;28(8):1993-2003.
- Kim HY, Yang DH, Shin SW, et al. CXXC5 is a transcriptional activator of Flk-1 and mediates bone morphogenic protein-induced endothelial cell differentiation and vessel formation. *FASEB J*. 2014;28(2):615-626.
- Lee SH, Seo SH, Lee DH, Pi LQ, Lee WS, Choi KY. Targeting of CXXC5 by a competing peptide stimulates hair regrowth and wound-induced hair neogenesis. *J*

- Invest Dermatol. 2017;137(11):2260-2269.
51. Akel S, Petrow-Sadowski C, Laughlin MJ, Ruscetti FW. Neutralization of autocrine transforming growth factor-beta in human cord blood CD34(+)CD38(-)Lin(-) cells promotes stem-cell-factor-mediated erythropoietin-independent early erythroid progenitor development and reduces terminal differentiation. *Stem Cells*. 2003;21(5):557-567.
  52. Gao X, Lee HY, da Rocha EL, et al. TGF-beta inhibitors stimulate red blood cell production by enhancing self-renewal of BFU-E erythroid progenitors. *Blood*. 2016;128(23):2637-2641.
  53. Thompson NL, Flanders KC, Smith JM, Ellingsworth LR, Roberts AB, Sporn MB. Expression of transforming growth factor-beta 1 in specific cells and tissues of adult and neonatal mice. *J Cell Biol*. 1989;108(2):661-669.
  54. Carrancio S, Markovics J, Wong P, et al. An activin receptor IIA ligand trap promotes erythropoiesis resulting in a rapid induction of red blood cells and haemoglobin. *Br J Haematol*. 2014;165(6):870-882.
  55. Bewersdorf JP, Zeidan AM. Transforming growth factor (TGF)-beta pathway as a therapeutic target in lower risk myelodysplastic syndromes. *Leukemia*. 2019;33(6):1303-1312.
  56. Fenaux P, Kiladjian JJ, Platzbecker U. Luspatercept for the treatment of anemia in myelodysplastic syndromes and primary myelofibrosis. *Blood*. 2019;133(8):790-794.
  57. Suragani RN, Cawley SM, Li R, et al. Modified activin receptor IIB ligand trap mitigates ineffective erythropoiesis and disease complications in murine beta-thalassemia. *Blood*. 2014;123(25):3864-3872.
  58. Lio CJ, Yuita H, Rao A. Dysregulation of the TET family of epigenetic regulators in hematopoietic malignancies. *Blood*. 2019;134(18):1487-1497.
  59. Yan H, Wang Y, Qu X, et al. Distinct roles for TET family proteins in regulating human erythropoiesis. *Blood*. 2017;129(14):2002-2012.
  60. Gelsi-Boyer V, Trouplin V, Adelaide J, et al. Mutations of polycomb-associated gene ASXL1 in myelodysplastic syndromes and chronic myelomonocytic leukaemia. *Br J Haematol*. 2009;145(6):788-800.
  61. Wei L, Zhao S, Wang G, et al. SMAD7 methylation as a novel marker in atherosclerosis. *Biochem Biophys Res Commun*. 2018;496(2):700-705.
  62. Yang Q, Chen HY, Wang JN, et al. Alcohol promotes renal fibrosis by activating Nox2/4-mediated DNA methylation of Smad7. *Clin Sci (Lond)*. 2020;134(2):103-122.
  63. Bian EB, Huang C, Wang H, et al. Repression of Smad7 mediated by DNMT1 determines hepatic stellate cell activation and liver fibrosis in rats. *Toxicol Lett*. 2014;224(2):175-185.
  64. Itzykson R, Kosmider O, Cluzeau T, et al. Impact of TET2 mutations on response rate to azacitidine in myelodysplastic syndromes and low blast count acute myeloid leukemias. *Leukemia*. 2011;25(7):1147-1152.
  65. Yue L, Bartenstein M, Zhao W, et al. Efficacy of ALK5 inhibition in myelofibrosis. *JCI insight*. 2017;2(7):e90932.
  66. Zhang H, Kozono DE, O'Connor KW, et al. TGF-beta inhibition rescues hematopoietic stem cell defects and bone marrow failure in Fanconi anemia. *Cell Stem Cell*. 2016;18(5):668-681.
  67. Piga A, Perrotta S, Gamberini MR, et al. Luspatercept improves hemoglobin levels and blood transfusion requirements in a study of patients with beta-thalassemia. *Blood*. 2019;133(12):1279-1289.
  68. Verma A, Suragani RN, Aluri S, et al. Biological basis for efficacy of activin receptor ligand traps in myelodysplastic syndromes. *J Clin Invest*. 2020;130(2):582-589.
  69. Cheng W, Wang F, Feng A, Li X, Yu W. CXXC5 attenuates pulmonary fibrosis in a bleomycin-induced mouse model and MLFs by suppression of the CD40/CD40L pathway. *Biomed Res Int*. 2020;2020:7840652.